

Algebraic Geometry for Spin-Adapted Coupled Cluster Theory

Fabian M. Faulstich and Svala Sverrisdóttir

February 6, 2026

Abstract

We develop and numerically analyze an algebraic-geometric framework for spin-adapted coupled-cluster (CC) theory. Since the electronic Hamiltonian is $SU(2)$ -invariant, physically relevant quantum states lie in the spin singlet sector. We give an explicit description of the $SU(2)$ -invariant (spin singlet) many-body space by identifying it with an Artinian commutative ring, called the excitation ring, whose dimension is governed by a Narayana number. We define spin-adapted truncation varieties via embeddings of graded subspaces of this ring, and we identify the CCS truncation variety with the Veronese square of the Grassmannian. Compared to the spin-generalized formulation, this approach yields a substantial reduction in dimension and degree, with direct computational consequences. In particular, the CC degree of the truncation variety – governing the number of homotopy paths required to compute all CC solutions – is reduced by orders of magnitude. We present scaling studies demonstrating asymptotic improvements and we exploit this reduction to compute the full solution landscape of spin-adapted CC equations for water and lithium hydride.

1 Introduction

Interacting many-electron problems pose some of the greatest computational challenges in science, with essential applications across chemistry, materials science, and condensed-matter physics [1–9]. Scalable accurate solutions will enable predictive simulations of chemical reactivity and kinetics, as well as reliable access to ground- and excited-state properties of quantum systems. Coupled cluster (CC) theory is widely regarded as one of the most accurate general-purpose methods in electronic structure theory [10–17]. It is routinely used as a benchmark in method development [18–22] and as a target accuracy level for data-driven and machine-learning approaches [23–27].

The governing equations, called the *CC equations*, correspond to a system of polynomial equations [28–30]. Under certain assumptions, isolated roots of this system, called the *CC solutions*, can recover the exact eigenstates of the underlying electronic Hamiltonian within the chosen model space. Understanding the structure of this solution set, e.g., its size, multiplicities, and dependence on physical parameters, is therefore of computational as well

as physical interest. Yet, because of the high dimensionality and strong nonlinearity of the CC equations, many fundamental features of their solution landscapes remain undiscovered.

In this work, we extend recent algebraic investigations establishing a foundational understanding of the coupled-cluster solution set [31–33]. In particular, we here study *spin adaptation* and its effect on the structure and complexity of the CC equations [34]. Spin adaptation is central in quantum many-body applications: the conservation of total spin implies that the physically relevant states lie in prescribed spin sectors, e.g., singlets for closed-shell molecules [35]. Restricting the parameterization to spin-adapted excitations both enforces physical consistency and substantially simplifies the associated polynomial system, leading to significant computational speedups confirmed by our numerical results.

We develop an algebraic-geometric formulation of spin-adapted coupled cluster theory and use it to reduce the complexity of *fully* solving the CC equations in the physically relevant spin singlet sector. In Section 3 we study the $SU(2)$ -invariant space of the d -electron space $\mathcal{H}_d \cong \wedge^d \mathcal{H}$. We derive a closed formula for the dimensions of the total-spin sectors, including the $SU(2)$ -invariant subspace. We identify \mathcal{H}_d with a particle-number conserving subalgebra of the Fermi–Dirac algebra. There, spin adaptation becomes the restriction to $SU(2)$ -invariant cluster amplitudes. We prove that the space of invariant amplitudes is an Artinian commutative ring, called the excitation ring, generated by the *excitation operators*. In Section 4 we introduce the *spin singlet truncation varieties*. They are the Zariski closures of the projective images of graded subspaces of the excitation ring under the exponential map. We show that the singlet CCS truncation variety, consisting of $SU(2)$ -invariant Slater determinants, is the Veronese square of the Grassmannian. The truncation varieties provide a geometric framework for formulating the spin-adapted CC equations. We offer an upper bound of the CC degree (general solution count for the CC equations) in terms of invariants of the truncation varieties; and we find the explicit CC degree for the 2nd Veronese variety.

In Section 5 we illustrate the computational improvements of these structural results. The CC degree determines the number of continuation paths in homotopy-based solvers, therefore restricting to $SU(2)$ -invariants collapses the generic root count while targeting *spin-pure solutions*. We compare the CC degrees of the spin-adapted CC equations with those of the spin-generalized formulation, revealing dramatic reductions by orders of magnitude. We compute the full solution spectrum of the singlet CCD equations for lithium hydrate (LiH) and water (H_2O) in a minimal-basis. Numerically, the speedup is already substantial for small systems, enabling systematic *algebro-computational* investigations of coupled-cluster solution landscapes that were computationally out of reach in the spin-generalized formulations.

1.1 Previous Works and Perspective

The first systematic study of the root structure of coupled cluster (CC) equations dates back to 1978, when Živković and Monkhorst analyzed singularities and multiple solutions in single-reference CC theory [36]. In the early 1990s, Paldus and coauthors developed further mathematical and numerical analyses of the solution manifolds of single-reference and state-universal multireference CC equations, including their singularities and analytic properties [37, 38]. Homotopy methods were revived in the CC context by Kowalski and

Jankowski, who solved a CCD system in [39]; Kowalski and Piecuch subsequently extended these ideas to CCSD, CCSDT, and CCSDTQ for a four-electron minimal-basis model [40]. These works led to the β -nested equations and the *Fundamental Theorem of the β -NE Formalism* [41], which explains how solution branches connect across truncation levels (e.g., CCSD \rightarrow CCSDT \rightarrow CCSDTQ). The resulting *Kowalski–Piecuch homotopy* has recently been analyzed in depth using topological degree theory [42, 43]. Related homotopy-based studies produced complete solution sets of the generalized Bloch equation [44] and clarified symmetry-breaking mechanisms within CC theory [45–49].

A more explicitly algebraic and mathematically driven line of work has recently gained momentum. Initiated by some of the present authors, an algebraic perspective on CC theory was introduced in [31], and subsequent in-depth analysis led to the algebraic framework of CC truncation varieties [32]. This viewpoint has since motivated a sequence of contributions ranging from pure mathematics [50, 51] to domain applications [33]. More broadly, these developments reflect a growing interest in a rigorous mathematical understanding of CC theory within the pure and applied mathematics community. In this context, Schneider gave the first local analysis of CC theory in 2009 using functional-analytic techniques [52]; this framework was generalized in [53, 54] and extended to additional CC variants in [55–57]. A complementary and more flexible approach based on topological degree theory was later proposed by Csirik and Laestadius [42, 43]. The most recent numerical-analysis results for single-reference CC were obtained by Hassan, Maday, and Wang [58, 59]. For a comprehensive review of the recent mathematical advances, we refer the interested reader to [60]. Beyond the direct applications to coupled cluster theory, algebro computational approaches find more and more use in electronic structure theory [61–65].

1.2 Notational Preamble

Throughout this manuscript, m denotes the number of spatial orbitals and $n = 2m$ the number of spin orbitals. We generally consider a closed-shell system with $d = 2k$ electrons (k electron pairs). We use $[m] := \{1, \dots, m\}$ and denote $\llbracket m \rrbracket := [m] \times \{\uparrow, \downarrow\}$. Operators in the Fermi–Dirac algebra $\text{FD}_{2m} \cong \text{End}(\mathcal{F})$ carry hats.

2 The Electronic Structure Problem

The *electronic Schrödinger equation* describing d electrons in the electromagnetic field generated by d_{nuc} fixed nuclei is the eigenvalue problem

$$\mathcal{H} \psi(\mathbf{x}_1, \mathbf{x}_2, \dots, \mathbf{x}_d) = \lambda \psi(\mathbf{x}_1, \mathbf{x}_2, \dots, \mathbf{x}_d), \quad (1)$$

where the unknown *wave function* $\psi(\mathbf{x}_1, \mathbf{x}_2, \dots, \mathbf{x}_d)$ fully characterizes the physical system [66]. Here $\mathbf{x}_i = (\mathbf{r}_i, \sigma_i) \in \mathbb{R}^3 \times \{\uparrow, \downarrow\}$ denotes the spatial coordinate \mathbf{r}_i and spin coordinate σ_i of the i th electron. The Pauli principle requires ψ to be skewsymmetric under exchange of any two electron coordinates (vide infra), and we view ψ as a sufficiently smooth element of the skewsymmetric subspace of $L^2((\mathbb{R}^3 \times \{\uparrow, \downarrow\})^d)$. In atomic units, the electronic

Hamiltonian \mathcal{H} in Eq. (1) is the differential operator

$$\mathcal{H} := -\frac{1}{2} \sum_{i=1}^d \Delta_{\mathbf{r}_i} - \sum_{i=1}^d \sum_{j=1}^{d_{\text{nuc}}} \frac{Z_j}{|\mathbf{r}_i - \mathbf{R}_j|} + \sum_{1 \leq i < j \leq d} \frac{1}{|\mathbf{r}_i - \mathbf{r}_j|}. \quad (2)$$

We denote the Laplacian in \mathbf{r}_i by $\Delta_{\mathbf{r}_i}$, and all remaining terms in Eq. (2) act on ψ by multiplication. The nuclei are indexed by $j \in [d_{\text{nuc}}]$. The constant $Z_j \in \mathbb{N}$ is the charge (atomic number) of the j th nucleus, and its position $\mathbf{R}_j \in \mathbb{R}^3$ is fixed under the Born–Oppenheimer approximation [67]. Throughout, we consider charge-neutral molecules, i.e., $d = \sum_{j=1}^{d_{\text{nuc}}} Z_j$. Note that any nucleus–nucleus repulsion term is a constant for fixed $\{\mathbf{R}_j\}$ and may be added to \mathcal{H} without changing the structure of the electronic eigenvalue problem.

Electrons possess an intrinsic angular momentum called *spin* [68]. In the non-relativistic Born–Oppenheimer model considered here, spin does not appear explicitly in the differential operator in Eq. (2). However, it enters the *state space* and the admissibility condition (Pauli principle) in the following way: The physical d -electron wave function is a map

$$\psi : (\mathbb{R}^3)^d \times \{\uparrow, \downarrow\}^d \rightarrow \mathbb{C}; (\mathbf{r}, \boldsymbol{\sigma}) \mapsto \psi(\mathbf{r}, \boldsymbol{\sigma}), \quad (3)$$

i.e., it depends on spatial coordinates $\mathbf{r} = (\mathbf{r}_1, \dots, \mathbf{r}_d)$ and spin labels $\boldsymbol{\sigma} = (\sigma_1, \dots, \sigma_d)$. Pauli’s exclusion principle [69] states that admissible states are *skewsymmetric under simultaneous exchange* of position and spin, i.e., for every permutation P of the electrons,

$$\psi(P\mathbf{r}, P\boldsymbol{\sigma}) = \text{sign}(P) \psi(\mathbf{r}, \boldsymbol{\sigma}). \quad (4)$$

In particular, two electrons with equal spin cannot occupy the same position.

To discretize the Hamiltonian in Eq. (1), we require a finite-dimensional basis. Since the Hamiltonian does not explicitly depend on the electronic spin, we can impose a product basis. To that end, we first introduce the one-electron *spin space* $\mathcal{H}_{\text{spin}} \cong \mathbb{C}^2$ with orthonormal basis $\{e_\uparrow, e_\downarrow\}$ (spin up/down). Second, we introduce an orthonormal set of spatial basis functions (orbitals) $\{\varphi_p\}_{p=1}^m \subset H^1(\mathbb{R}^3)$. Each spatial orbital gives rise to two spin-orbitals

$$\phi_{p\uparrow}(\mathbf{r}, \sigma) := \varphi_p(\mathbf{r}) \delta_{\sigma, \uparrow}, \quad \phi_{p\downarrow}(\mathbf{r}, \sigma) := \varphi_p(\mathbf{r}) \delta_{\sigma, \downarrow}. \quad (5)$$

The spin-orbitals span the one-particle space \mathcal{H} , with $\mathcal{H} \cong \mathbb{C}^m \otimes \mathbb{C}^2$ and $\dim(\mathcal{H}) = n = 2m$. The Galerkin space of skewsymmetric d -electron functions is given by $\mathcal{H}_d \cong \wedge^d \mathcal{H}$, spanned by the canonical skewsymmetric product basis, i.e., the d -electron Slater determinants.

2.1 Second Quantization and Fermi Dirac Algebra

Discretizing the Hamiltonian in the skewsymmetric d -electron space $\wedge^d \mathcal{H}$ is known as *first quantization*. While conceptually direct, the resulting operators act on a high-dimensional tensor product and quickly become cumbersome to manipulate. An equivalent and more flexible viewpoint is obtained by working in the fermionic Fock space and representing observables as polynomials in creation and annihilation operators, i.e., *second quantization* [70].

Subsequently, we use the explicit basis $e_\downarrow = -e_2$, $e_\uparrow = e_1$ for $\mathcal{H}_{\text{spin}}$, where e_1 and e_2 form the standard basis of \mathbb{C}^2 and we denote the standard basis vectors of \mathbb{C}^m by e_p with $p \in [m]$. For notational convenience, we define $\llbracket m \rrbracket := [m] \times \{\downarrow, \uparrow\}$, with $n = 2m$ elements. Hence, a basis of \mathcal{H} is given by $e_{p\alpha} := e_p \otimes e_\alpha$, $(p, \alpha) \in \llbracket m \rrbracket$. The associated fermionic Fock space is the full exterior algebra

$$\mathcal{F} \cong \bigwedge \mathcal{H} = \bigoplus_{\ell=0}^n \bigwedge^\ell \mathcal{H}, \quad (6)$$

with canonical exterior basis vectors $e_I := \wedge_{(p,\alpha) \in I} e_{p\alpha}$ indexed by sets $I \subseteq \llbracket m \rrbracket$. For each basis element $e_{p\alpha} \in \mathcal{H}$ we define the creation and annihilation operators as the following exterior and interior products on \mathcal{F} :

$$\hat{a}_{p\alpha}^\dagger : \mathcal{F} \rightarrow \mathcal{F}; \quad \psi \mapsto e_{p\alpha} \wedge \psi \quad \text{and} \quad \hat{a}_{p\alpha} : \mathcal{F} \rightarrow \mathcal{F}; \quad \psi \mapsto e_{p\alpha} \lrcorner \psi. \quad (7)$$

Here, \lrcorner is the dual operation to the wedge product \wedge , see [71, Section 3.6] and [51] for further explanation. These operators satisfy the canonical anticommutation relations (CAR), i.e.,

$$[\hat{a}_{p\alpha}^\dagger, \hat{a}_{q\beta}^\dagger]_+ = 0, \quad [\hat{a}_{p\alpha}, \hat{a}_{q\beta}]_+ = 0, \quad [\hat{a}_{p\alpha}^\dagger, \hat{a}_{q\beta}]_+ = \delta_{p,q} \delta_{\alpha,\beta}, \quad (8)$$

where $[\cdot, \cdot]_+$ denotes the anti-commutator. Note that the CAR implement Pauli's exclusion principle at the operator level, since $(\hat{a}_{p\alpha}^\dagger)^2 = 0$.

The *Fermi–Dirac algebra* FD_{2m} is the noncommutative algebra generated by the $4m$ creation and annihilation operators subject to the CAR in Eq. (8). Equivalently,

$$\text{FD}_{2m} := \mathbb{C} \left\langle \hat{a}_{1\downarrow}, \hat{a}_{1\uparrow}, \dots, \hat{a}_{m\downarrow}, \hat{a}_{m\uparrow}, \hat{a}_{1\downarrow}^\dagger, \hat{a}_{1\uparrow}^\dagger, \dots, \hat{a}_{m\downarrow}^\dagger, \hat{a}_{m\uparrow}^\dagger \right\rangle \Big/ \langle G \rangle,$$

where G denotes the set of relations from Eq. (8). Using the creation and annihilation operators, we can discretize the Hamiltonian in Eq. (2) over \mathcal{F} [68, 72], i.e.,

$$\hat{H} = \sum_{pq,\sigma} h_{pq} \hat{a}_{p\sigma}^\dagger \hat{a}_{q\sigma} + \frac{1}{2} \sum_{pqrs} \sum_{\sigma\tau} v_{pqrs} \hat{a}_{p\sigma}^\dagger \hat{a}_{r\tau}^\dagger \hat{a}_{s\tau} \hat{a}_{q\sigma}, \quad (9)$$

where h_{pq} and v_{pqrs} are one- and two-electron integrals over spatial orbitals,

$$h_{pq} := \int \varphi_p^*(\mathbf{r}) \left(-\frac{1}{2} \Delta - \sum_j \frac{Z_j}{\|\mathbf{r} - \mathbf{R}_j\|} \right) \varphi_q(\mathbf{r}) d\mathbf{r}, \quad (10)$$

$$v_{pqrs} := \iint \varphi_p^*(\mathbf{r}_1) \varphi_q(\mathbf{r}_1) \frac{1}{\|\mathbf{r}_1 - \mathbf{r}_2\|} \varphi_r(\mathbf{r}_2)^* \varphi_s(\mathbf{r}_2) d\mathbf{r}_1 d\mathbf{r}_2. \quad (11)$$

Since its monomials contain equal numbers of creation and annihilation operators, \hat{H} conserves particle number and may be restricted to an endomorphism of the d th exterior power

$$\mathcal{H}_d \cong \bigwedge^d \mathcal{H} \subset \mathcal{F}. \quad (12)$$

Remark 2.1. Wick’s theorem states that G forms a Gröbner basis for the Fermi–Dirac algebra, with respect to degree lexicographic order [51, Theorem 2.5]. Therefore, the Fermi–Dirac algebra is isomorphic to a 2^{4m} -dimensional vector space generated by the *standard monomials*, also known as the normal ordered strings of ladder operators [73, 74]. Every element in FD_{2m} can be written as a linear combination of them, called the *standard representation*.

Elements of the Fermi–Dirac algebra are endomorphisms of \mathcal{F} and, by dimension counting, we see that, as a vector space, the Fermi–Dirac algebra is isomorphic to $\text{End}(\mathcal{F})$. Moreover, the Fermi–Dirac algebra admits a natural \mathbb{Z}^2 -grading, by setting $\deg(a_{p\alpha}^\dagger) = e_1$ and $\deg(a_{p\alpha}) = e_2$. This bidegree coincides with the *annihilation and creation levels* introduced in [51, Section 3]. Subsequently, we assume particle–number conservation and restrict attention to the subalgebra generated by elements of bidegree (ℓ, ℓ) for $1 \leq \ell \leq m$, which we refer to as having *excitation level* ℓ . As a vector space, this subalgebra is isomorphic to

$$\text{End}(\mathcal{H}_0) \oplus \text{End}(\mathcal{H}_1) \oplus \cdots \oplus \text{End}(\mathcal{H}_n), \quad \mathcal{H}_\ell := \wedge^\ell \mathcal{H}. \quad (13)$$

3 Representations of the Fermi–Dirac Algebra

The electronic spin can be viewed as a two-dimensional internal degree of freedom of each electron [35, 68]. In the non-relativistic Born–Oppenheimer setting (i.e., in the absence of spin–orbit and magnetic-field terms), the electronic-structure Hamiltonian \hat{H} in Eq. (9) is $\text{SU}(2)$ -invariant (i.e., spin-rotationally invariant) and hence commutes with the total-spin operators \hat{S}^2 and \hat{S}_z (vide infra), so that the Hilbert space decomposes into spin sectors (e.g., singlets, triplets, etc.) [35]. For spin- $\frac{1}{2}$ the relevant symmetry group is not $\text{SO}(3)$ itself but its double cover $\text{SU}(2)$, whose defining representation acts on the spin space $\mathcal{H}_{\text{spin}} \cong \mathbb{C}^2$ [35, 68, 75]. To exploit this symmetry in many-electron computations, we study the induced $\text{SU}(2)$ -action on the skewsymmetric d -electron space and, equivalently, on the operator algebra in second quantization. This provides a precise algebraic notion of spin invariance and allows us to isolate, in particular, the singlet sector used in spin-adapted formulations [76]. The argument uses two standard facts. First, differentiation induces a one-to-one correspondence between finite-dimensional representations of $\text{SU}(2)$ and finite-dimensional representations of $\mathfrak{su}(2)$. Indeed, because $\text{SU}(2)$ is simply connected, every finite-dimensional $\mathfrak{su}(2)$ -representation integrates to $\text{SU}(2)$ (cf. [77, Exercise 8.10]). Second, complex representations of $\mathfrak{su}(2)$ are in one-to-one correspondence with representations of $\mathfrak{sl}_2(\mathbb{C})$ via complexification, since $\mathfrak{su}(2) \otimes_{\mathbb{R}} \mathbb{C} \cong \mathfrak{sl}_2(\mathbb{C})$.

3.1 Spin of a Single Electron

Recall that the Lie algebra $\mathfrak{su}(2)$ consists of traceless skew-Hermitian 2×2 matrices,

$$\mathfrak{su}(2) = \{A \in \mathbb{C}^{2 \times 2} : A^* = -A, \text{tr}(A) = 0\}. \quad (14)$$

The three 2×2 matrices $(\frac{i}{2}\sigma_x, \frac{i}{2}\sigma_y, \frac{i}{2}\sigma_z)$, where $\sigma_x, \sigma_y, \sigma_z$ are the Pauli matrices [78], form a basis for $\mathfrak{su}(2)$. Similarly, it is common to work with the associated Hermitian operators,

i.e., $S_x = \frac{1}{2}\sigma_x$, $S_y = \frac{1}{2}\sigma_y$, and $S_z = \frac{1}{2}\sigma_z$, noting that $-iS_x, -iS_y, -iS_z \in \mathfrak{su}(2)$ and that spin rotations are given by $\exp(-i\theta_x S_x - i\theta_y S_y - i\theta_z S_z) \in \mathrm{SU}(2)$. For our purposes, it is convenient to work with the associated spin ladder operators, i.e.,

$$S_+ = S_x + iS_y = \frac{1}{2}(\sigma_x + i\sigma_y), \quad S_- = S_x - iS_y = \frac{1}{2}(\sigma_x - i\sigma_y), \quad S_z = \frac{1}{2}\sigma_z, \quad (15)$$

where S_z is diagonal in the $\{\uparrow, \downarrow\}$ basis and hence directly encodes the spin projection, while S_+ and S_- act as raising and lowering operators, i.e., flipping “ $\downarrow \mapsto \uparrow$ ” and “ $\uparrow \mapsto \downarrow$ ”, respectively. Note that S_\pm are not elements of $\mathfrak{su}(2)$ but lie in its complexification $\mathfrak{sl}_2(\mathbb{C})$. Moreover, a central operator for the discussion of spin symmetry is the *total-spin operator*

$$S^2 := S_x^2 + S_y^2 + S_z^2 = S_z^2 + \frac{1}{2}(S_+S_- + S_-S_+). \quad (16)$$

Remark 3.1. The finite-dimensional irreducible representations of $\mathrm{SU}(2)$ are parametrized by non-negative half-integers: for each $j \in \frac{1}{2}\mathbb{Z}_{\geq 0}$ there is an irreducible representation $V_j \cong \mathrm{Sym}^{2j}(\mathbb{C}^2)$, see [77, Section 11.1]. The space $\mathrm{Sym}^{2j}(\mathbb{C}^2)$ can be realized as the space of homogeneous polynomials in two variables x, y of degree $2j$. It has the monomial basis $\{x^{2j-i}y^i \mid 0 \leq i \leq 2j\}$, and hence $\dim V_j = 2j + 1$. The $\mathrm{SU}(2)$ -action on V_j is the induced action on homogeneous polynomials coming from left multiplication of the variable vector.

The irreducible representation of $\mathrm{SU}(2)$ on $V_{\frac{1}{2}} \cong \mathbb{C}^2$ is called the spin- $\frac{1}{2}$ representation. Differentiation yields the corresponding representation of the Lie algebra $\mathfrak{su}(2)$, commonly referred to as the fundamental representation. We define an $\mathfrak{su}(2)$ -action on the spin space $\mathcal{H}_{\mathrm{spin}} \cong \mathbb{C}^2 \cong V_{\frac{1}{2}}$ by describing the action of the generators on the basis vectors, i.e.

$$\begin{aligned} S_+(e_\downarrow) &= -e_\uparrow & S_-(e_\downarrow) &= 0 & S_z(e_\downarrow) &= -\frac{1}{2}e_\downarrow \\ S_+(e_\uparrow) &= 0 & S_-(e_\uparrow) &= -e_\downarrow & S_z(e_\uparrow) &= \frac{1}{2}e_\uparrow. \end{aligned} \quad (17)$$

See equations (3.10)–(3.12) in [75, Section 3.2]. In the explicit basis $e_\downarrow = -e_2$, $e_\uparrow = e_1$ this action coincides with left multiplication: for $g \in \mathfrak{su}(2)$ it acts on $\mathcal{H}_{\mathrm{spin}}$ by $v \mapsto gv$.

We can extend this action to an $\mathfrak{su}(2)$ -action on the one-particle space \mathcal{H} by acting only on the spin factor, i.e., $g(e_{p\alpha}) = e_p \otimes g e_\alpha$ for $g \in \mathfrak{su}(2)$. Equivalently, in the basis $\{e_{p\alpha}\}_{(p,\alpha) \in \llbracket m \rrbracket}$ the action is represented by

$$g_m := I_m \otimes g \in \mathbb{C}^{(2m) \times (2m)} \cong \mathbb{C}^{n \times n}. \quad (18)$$

Note that this representation is reducible.

3.2 Spin of d -Electron States and Spin-Singlet d -Electron States

We further induce the $\mathfrak{su}(2)$ -action onto the space \mathcal{H}_d of d -particle states, canonically via

$$g(e_I) := \sum_{r=1}^d e_{i_1\alpha_1} \wedge \cdots \wedge g(e_{i_r\alpha_r}) \wedge \cdots \wedge e_{i_d\alpha_d}. \quad (19)$$

In the exterior basis $\{e_I : |I| = d\}$ of \mathcal{H}_d , the action is represented by a $\binom{n}{d} \times \binom{n}{d}$ matrix acting by left multiplication on the coordinate vectors:

$$g^{(d)} := \sum_{k=1}^d \underbrace{I_{\mathcal{H}} \wedge \dots \wedge I_{\mathcal{H}}}_{k-1 \text{ times}} \wedge g_m \wedge \underbrace{I_{\mathcal{H}} \wedge \dots \wedge I_{\mathcal{H}}}_{d-k \text{ times}} \in \text{End}(\mathcal{H}_d). \quad (20)$$

The space of *total-spin singlet states* (or simply *spin singlets*) $\mathcal{H}_d^{\text{SU}(2)}$ is defined by the quantum states that are invariant under the natural $\text{SU}(2)$ -action on the spin factor, or equivalently, the quantum states that are mapped to zero by the derived $\mathfrak{su}(2)$ -action (cf. (19)). We can describe this $\text{SU}(2)$ -invariant subspace explicitly by

$$\mathcal{H}_d^{\text{SU}(2)} := \{\psi \in \mathcal{H}_d : S_z^{(d)}\psi = S_+^{(d)}\psi = S_-^{(d)}\psi = 0\}. \quad (21)$$

Alternatively, we define the space of spin singlets as the eigenspace of S^2 with eigenvalue 0:

$$\mathcal{H}_d^{\text{SU}(2)} = \{\psi \in \mathcal{H}_d : (S^{(d)})^2 \psi = 0\}. \quad (22)$$

We see that by definition of $(S^{(d)})^2$, Eq. (21) implies Eq. (22). For the inverse, recall that $S_x^{(d)}$, $S_y^{(d)}$, and $S_z^{(d)}$ are self-adjoint and therefore

$$\begin{aligned} \langle \psi, (S^{(d)})^2 \psi \rangle &= \langle \psi, (S_x^{(d)})^2 \psi \rangle + \langle \psi, (S_y^{(d)})^2 \psi \rangle + \langle \psi, (S_z^{(d)})^2 \psi \rangle \\ &= \|S_x^{(d)}\psi\|^2 + \|S_y^{(d)}\psi\|^2 + \|S_z^{(d)}\psi\|^2 \geq 0. \end{aligned} \quad (23)$$

Hence, $\psi \in \ker((S^{(d)})^2)$ implies $S_x^{(d)}\psi = S_y^{(d)}\psi = S_z^{(d)}\psi = 0$ and consequently $S_{\pm}^{(d)}\psi = 0$. More generally, the total-spin operator $(S^{(d)})^2$ is the Casimir operator of the induced $\mathfrak{su}(2)$ -action [79]. Consequently, it acts on \mathcal{H}_d by multiplication of a scalar. In particular, we define the spin- s sector as the subspace of \mathcal{H}_d where

$$(S^{(d)})^2 \psi = s(s+1) \psi. \quad (24)$$

For $s = 0, \frac{1}{2}, 1, \frac{3}{2}, \dots$, these spaces are referred to as the spin singlet, doublet, triplet, quartet, and higher spin sectors, respectively. For example, the spin triplet sector is the eigenspace of $(S^{(d)})^2$ corresponding to eigenvalue 2. This yields a canonical decomposition of \mathcal{H}_d into irreducible spin sectors. The electronic Hamiltonian in Eq. (9) is $\text{SU}(2)$ -invariant and hence it commutes with $(S^{(d)})^2$, and therefore preserves the decomposition. Computations are thus typically carried out within a fixed sector – in this paper, the spin singlet sector.

From a representation-theoretic viewpoint, the singlet sector corresponds to the trivial representation V_0 of $\text{SU}(2)$, which is 1-dimensional and consists of $\text{SU}(2)$ -invariant vectors (equivalently, vectors annihilated by the derived $\mathfrak{su}(2)$ -action). The space \mathcal{H}_d is completely reducible as an $\text{SU}(2)$ -module. Hence it decomposes into irreducibles with multiplicities,

$$\mathcal{H}_d \cong \bigoplus_{j \in \frac{1}{2}\mathbb{Z}_{\geq 0}} V_j^{\oplus c_j}, \quad (25)$$

where V_j denotes the j th irreducible $SU(2)$ -representation, defined in Remark 3.1. In this decomposition, the spin singlet sector is exactly the $j = 0$ isotypic component,

$$\mathcal{H}_d^{\text{SU}(2)} \cong V_0^{c_0} \cong \mathbb{C}^{c_0}. \quad (26)$$

Equivalently, the spin- s sectors are isomorphic to the s isotypic components $V_s^{\oplus c_s}$ [79].

Remark 3.2. In quantum chemistry, “spin-restricted” refers to a constraint at the one-particle (orbital) level, e.g., in spin-restricted Hartree-Fock theory, the α and β electrons share the same spatial orbitals. In particular, spin-restricted is primarily a statement about the reference and orbital parametrization, not about the symmetry content of a correlated ansatz. By contrast, *spin-adapted* (i.e., $SU(2)$ -adapted) refers to the *many-electron* level: the wavefunction (or equivalently the operator ansatz acting on a reference) is constructed to transform in a fixed irreducible $SU(2)$ -representation. Thus, “restricted” and “adapted” address different levels of theory (i.e., orbitals vs. many-body symmetry) and are logically independent. A restricted reference does not by itself enforce $SU(2)$ adaptation of a correlation ansatz, whereas $SU(2)$ adaptation explicitly restricts the state to a chosen spin sector.

Remark 3.3. We note that $\mathcal{H}_d^{\text{SU}(2)} \neq \{0\}$ only when d is even, e.g., $d = 2k$. An exterior basis vector $e_{I\uparrow} \wedge e_{J\downarrow}$ of \mathcal{H}_d (with $|I| + |J| = d$) is an eigenvector of $S_z^{(d)}$. Here, each spin-up (“ \uparrow ”) contributes $+\frac{1}{2}$ to the eigenvalue and each spin-down (“ \downarrow ”) contributes $-\frac{1}{2}$. Explicitly,

$$S_z^{(d)}(e_{I\uparrow} \wedge e_{J\downarrow}) = \frac{1}{2}(|I| - |J|) e_{I\uparrow} \wedge e_{J\downarrow}. \quad (27)$$

If $\psi \in \mathcal{H}_d^{\text{SU}(2)}$, then in particular $S_z^{(d)}\psi = 0$, so ψ can have support only on basis vectors with $|I| = |J|$ enforcing $d = |I| + |J| = 2|J|$. Therefore $\ker(S_z^{(d)}) = \{0\}$ for odd d , and, consequently, $\mathcal{H}_d^{\text{SU}(2)} \subseteq \ker(S_z^{(d)})$ implies $\mathcal{H}_d^{\text{SU}(2)} = \{0\}$ whenever d is odd.

Remark 3.4 (Proper embeddings of $\mathcal{H}_d^{\text{SU}(2)}$). Note that the condition $S_z\psi = 0$ alone selects the sector $\ker(S_z) \subset \mathcal{H}_d$, isomorphic to $\wedge^k \mathbb{C}^m \otimes \wedge^k \mathbb{C}^m$ via $e_{I\uparrow} \wedge e_{J\downarrow} \mapsto e_I \otimes e_J$. Since $\ker(S_z)$ generally contains contributions from higher-spin irreducibles, we obtain a proper embedding

$$\mathcal{H}_d^{\text{SU}(2)} \subsetneq \ker(S_z) \cong \wedge^k \mathbb{C}^m \otimes \wedge^k \mathbb{C}^m. \quad (28)$$

In particular, the conditions $S_{\pm}\psi = 0$ enforce the spin-up and spin-down orbitals to be isomorphic. Therefore, we instead consider the symmetric power $\text{Sym}_2(\wedge^k \mathbb{C}^m)$, which has dimension $\binom{m}{k} + 1$. This space is isomorphic to the subspace of \mathcal{H}_d generated by

$$e_{J\uparrow} \wedge e_{J\downarrow}, \quad e_{J\uparrow} \wedge e_{K\downarrow} + (-1)^{|J \setminus K|} e_{K\uparrow} \wedge e_{J\downarrow}, \quad (29)$$

where $J < K \in \binom{[n]}{k}$ are distinct subsets of size k . This symmetry, however, still does not enforce $SU(2)$ -invariance: the above generators need not vanish under the action of S_{\pm} . For example, when $k = 2$, consider the vector

$$\psi = e_{1\uparrow} \wedge e_{2\uparrow} \wedge e_{3\downarrow} \wedge e_{4\downarrow} + e_{1\downarrow} \wedge e_{2\downarrow} \wedge e_{3\uparrow} \wedge e_{4\uparrow}. \quad (30)$$

Here, $\psi \in \text{Sym}_2(\wedge^k \mathbb{C}^m)$, but $S_+ \psi \neq 0$. Hence $\mathcal{H}_d^{\text{SU}(2)}$ is also a proper subspace of $\text{Sym}_2(\wedge^k \mathbb{C}^m)$ and determining the invariant space itself requires more refined tools. Nonetheless, the proper embedding of the invariant space $\mathcal{H}_d^{\text{SU}(2)}$ into $\text{Sym}_2(\wedge^k \mathbb{C}^m)$ will be useful in Section 4, as the larger space exhibits a simpler structure than the invariant space itself.

We analyze the irreducible decomposition of the $\text{SU}(2)$ -representation \mathcal{H}_d using characters. Recall that the *character* of a finite-dimensional complex representation V of $\text{SU}(2)$ is the class function

$$\chi_V : \text{SU}(2) \rightarrow \mathbb{C} ; g \mapsto \text{Tr}(g|_V) . \quad (31)$$

Here, $g|_V$ denotes the map $V \rightarrow V$ defined by a 2×2 matrix $g \in \text{SU}(2)$, and $\text{Tr}(g|_V)$ is the trace of the corresponding matrix of size $\dim(V)$. The character χ_V is constant on conjugacy classes [80, Chapter 10]. Since every $U \in \text{SU}(2)$ is unitary (hence normal), it is conjugate in $\text{SU}(2)$ to an element of the maximal torus

$$\mathbb{T} := \{ \text{diag}(z, z^{-1}) : |z| = 1 \} \cong S^1 . \quad (32)$$

Ergo, characters of $\text{SU}(2)$ are determined by their restriction to \mathbb{T} . It is therefore convenient to write $\chi_V(z) := \chi_V(\text{diag}(z, z^{-1}))$, so that χ_V is a Laurent polynomial with finite support. Moreover, since $t \in \mathbb{T}$ is conjugate with t^{-1} , the Weyl symmetry $\chi_V(z) = \chi_V(z^{-1})$ holds.

The irreducible representations of $\text{SU}(2)$ are indexed by $j \in \frac{1}{2}\mathbb{Z}_{\geq 0}$ and may be realized as $V_j \cong \text{Sym}^{2j}(\mathbb{C}^2)$. The action of $t = \text{diag}(z, z^{-1}) \in \mathbb{T}$ on $\text{Sym}^{2j}(\mathbb{C}^2)$ is diagonal in the standard monomial basis, with eigenvalues $z^{2j}, z^{2j-2}, \dots, z^{-2j}$. Hence, the irreducible character is

$$\chi_j(z) = \text{Tr} \left(t|_{V_j} \right) = \sum_{i=0}^{2j} z^{2j-2i} = z^{2j} + z^{2j-2} + \dots + z^{-2j} . \quad (33)$$

In particular, $\chi_{1/2}(z) = z + z^{-1}$. These characters are linearly independent and, by [77, Proposition 2.1], an irreducible decomposition $V \cong \bigoplus_j V_j^{\oplus c_j}$ implies the character identity

$$\chi_V(z) = \sum_j c_j \chi_j(z) . \quad (34)$$

Thus the multiplicities c_j (and in particular $c_0 = \dim(\mathcal{H}_d^{\text{SU}(2)})$) can be recovered by decomposing χ_V in the basis $\{\chi_j\}_j$ of irreducible characters.

Lemma 3.5. *The character of the representation \mathcal{H}_d of $\text{SU}(2)$ is the Laurent polynomial*

$$\chi_{\mathcal{H}_d}(z) = \sum_{i=0}^d \binom{m}{i} \binom{m}{d-i} z^{d-2i} . \quad (35)$$

If $d = 2k$ then \mathcal{H}_d decomposes into a sum of integer irreducible representations V_j where $0 \leq j \leq k$, with multiplicity

$$c_j = \binom{m}{k-j} \binom{m}{k+j} - \binom{m}{k-j-1} \binom{m}{k+j+1} . \quad (36)$$

If $d = 2k + 1$ then \mathcal{H}_d decomposes into a sum of half-integer irreducible representations $V_{j+\frac{1}{2}}$ where $0 \leq j \leq k$ with multiplicity

$$c_{j+\frac{1}{2}} = \binom{m}{k-j} \binom{m}{k+j+1} - \binom{m}{k-j-1} \binom{m}{k+j+2}. \quad (37)$$

Proof. Note that on the one-particle space $\mathcal{H} \cong \mathbb{C}^m \otimes \mathbb{C}^2$, the element $\text{diag}(z, z^{-1}) \in \mathbb{T}$ acts as the $n \times n$ diagonal matrix

$$g_n(z) = \text{diag}(z, z^{-1}, z, z^{-1}, \dots, z, z^{-1}). \quad (38)$$

Hence, the character of $\mathcal{H}_d = \wedge^d \mathcal{H}$ is the trace of the d th exterior power of $g_n(z)$. Its diagonal entries are the principal $d \times d$ minors of $g_n(z)$, each obtained by selecting d diagonal entries of $g_n(z)$. Choosing i entries equal to z^{-1} and $d - i$ entries equal to z yields the monomial $z^{d-i}(z^{-1})^i = z^{d-2i}$, and the number of such choices is $\binom{m}{i} \binom{m}{d-i}$, proving Eq. (35).

We now decompose $\chi_{\mathcal{H}_d}$ into the irreducible characters in Eq. (33). We first assume $d = 2k$, and without loss of generality, we may assume $2k \leq m$. We determine the multiplicities recursively by matching the highest power of z . Write

$$\chi_{\mathcal{H}_d}(z) = \sum_{j \in \mathbb{Z}} a_j z^{2j}, \quad a_j = \binom{m}{k-j} \binom{m}{k+j}, \quad a_{-j} = a_j. \quad (39)$$

with the convention $\binom{m}{r} = 0$ for $r \notin \{0, \dots, m\}$. In particular, $a_j = 0$ for $j > k$, so the highest power occurring in $\chi_{\mathcal{H}_d}(z)$ is z^{2k} . Its coefficient is a_k , so we set $c_k := a_k$ and consider

$$\chi^{(1)}(z) := \chi_{\mathcal{H}_d}(z) - c_k \chi_k(z). \quad (40)$$

Since $\chi_{\mathcal{H}_d}$ is invariant under $z \mapsto z^{-1}$ and has nonnegative integer coefficients, the same holds for $\chi^{(1)}$. Moreover, the terms z^{2k} and z^{-2k} are removed, and the remaining highest term is $z^{2(k-1)}$ with coefficient c_{k-1} . Continuing downward, we find that the coefficient of z^{2j} in $\chi_{\mathcal{H}_d}(z)$ is $\sum_{\ell \geq j} c_\ell$, so the multiplicities satisfy

$$c_j = a_j - a_{j+1} = \binom{m}{k-j} \binom{m}{k+j} - \binom{m}{k-j-1} \binom{m}{k+j+1}. \quad (41)$$

Now, let $d = 2k + 1$. The character formula (35) becomes

$$\chi_{\mathcal{H}_{2k+1}}(z) = \sum_{j \in \mathbb{Z}} \binom{m}{k-j} \binom{m}{k+1+j} z^{2j+1}, \quad (42)$$

hence $\chi_{\mathcal{H}_{2k+1}}(z)$ is a Laurent polynomial with only odd exponents. Therefore, in the decomposition of \mathcal{H}_{2k+1} into irreducibles, only half-integer representations can occur. We determine the coefficients $c_{j+\frac{1}{2}}$ by the same triangular elimination as in the even case, matching the highest powers of z successively. This gives the formula in Eq. (37). \square

Theorem 3.6. For $d = 2k$ electrons in $n = 2m$ spin orbitals, the dimension of the spin singlet sector $\mathcal{H}_d^{\text{SU}(2)} \subsetneq \mathcal{H}_d$ is given by

$$\dim(\mathcal{H}_d^{\text{SU}(2)}) = N(m+1, k+1), \quad (43)$$

where $N(m+1, k+1)$ is a Narayana number (see A001263).

Proof. This is a direct consequence of Lemma 3.5 since

$$\dim(\mathcal{H}_d^{\text{SU}(2)}) = c_0 = \binom{m}{k}^2 - \binom{m}{k-1} \binom{m}{k+1} = \frac{1}{m+1} \binom{m+1}{k+1} \binom{m+1}{k} = N(m+1, k+1).$$

□

Remark 3.7. The Narayana numbers form a triangle of positive integers for $0 \leq k \leq m$ and refine the Catalan numbers via

$$\sum_{r=0}^m N(m+1, r+1) = C_{m+1}. \quad (44)$$

The Catalan number C_{m+1} counts Dyck paths from $(0,0)$ to $(2m+2,0)$, while the Narayana number $N(m+1, k+1)$ counts Dyck paths with exactly $k+1$ peaks (equivalently, k pits).

Example 3.8 ($2k = d = 4$; $2m = n = 8$). We consider 4 electrons in 4 spatial orbitals. Then $\mathcal{H}_4 \cong \wedge^4 \mathbb{C}^8$ has dimension $\dim(\mathcal{H}_4) = \binom{8}{4} = 70$ and Theorem 3.6 yields

$$\dim(\mathcal{H}_4^{\text{SU}(2)}) = N(5, 3) = 20. \quad (45)$$

The invariant space $\mathcal{H}_4^{\text{SU}(2)}$ is the intersection of the kernels of the three 70×70 matrices $S_z^{(d)}, S_+^{(d)}, S_-^{(d)}$ and it is generated by the following 20 vectors:

$$\begin{aligned} & e_{1\uparrow, 1\downarrow, 2\uparrow, 2\downarrow}, e_{1\uparrow, 1\downarrow, 2\downarrow, 3\uparrow} - e_{1\uparrow, 1\downarrow, 2\uparrow, 3\downarrow}, e_{1\downarrow, 2\uparrow, 2\downarrow, 3\uparrow} - e_{1\uparrow, 2\uparrow, 2\downarrow, 3\downarrow}, e_{1\uparrow, 1\downarrow, 3\uparrow, 3\downarrow}, \\ & e_{1\downarrow, 2\uparrow, 3\uparrow, 3\downarrow} - e_{1\uparrow, 2\downarrow, 3\uparrow, 3\downarrow}, e_{2\uparrow, 2\downarrow, 3\uparrow, 3\downarrow}, e_{1\uparrow, 1\downarrow, 2\downarrow, 4\uparrow} - e_{1\uparrow, 1\downarrow, 2\uparrow, 4\downarrow}, e_{1\downarrow, 2\uparrow, 2\downarrow, 4\uparrow} - e_{1\uparrow, 2\uparrow, 2\downarrow, 4\downarrow}, \\ & e_{1\uparrow, 1\downarrow, 3\downarrow, 4\uparrow} - e_{1\uparrow, 1\downarrow, 3\uparrow, 4\downarrow}, e_{1\downarrow, 2\uparrow, 3\downarrow, 4\uparrow} - e_{1\uparrow, 2\downarrow, 3\downarrow, 4\uparrow} - e_{1\downarrow, 2\uparrow, 3\uparrow, 4\downarrow} + e_{1\uparrow, 2\downarrow, 3\uparrow, 4\downarrow}, \\ & e_{2\uparrow, 2\downarrow, 3\downarrow, 4\uparrow} - e_{2\uparrow, 2\downarrow, 3\uparrow, 4\downarrow}, e_{1\downarrow, 2\downarrow, 3\uparrow, 4\uparrow} - e_{1\uparrow, 2\downarrow, 3\downarrow, 4\uparrow} - e_{1\downarrow, 2\uparrow, 3\uparrow, 4\downarrow} + e_{1\uparrow, 2\uparrow, 3\downarrow, 4\downarrow}, \\ & e_{1\downarrow, 3\uparrow, 3\downarrow, 4\uparrow} - e_{1\uparrow, 3\uparrow, 3\downarrow, 4\downarrow}, e_{2\downarrow, 3\uparrow, 3\downarrow, 4\uparrow} - e_{2\uparrow, 3\uparrow, 3\downarrow, 4\downarrow}, e_{1\uparrow, 1\downarrow, 4\uparrow, 4\downarrow}, e_{1\downarrow, 2\uparrow, 4\uparrow, 4\downarrow} - e_{1\uparrow, 2\downarrow, 4\uparrow, 4\downarrow}, \\ & e_{2\uparrow, 2\downarrow, 4\uparrow, 4\downarrow}, e_{1\downarrow, 3\uparrow, 4\uparrow, 4\downarrow} - e_{1\uparrow, 3\downarrow, 4\uparrow, 4\downarrow}, e_{2\downarrow, 3\uparrow, 4\uparrow, 4\downarrow} - e_{2\uparrow, 3\downarrow, 4\uparrow, 4\downarrow}, e_{3\uparrow, 3\downarrow, 4\uparrow, 4\downarrow}. \end{aligned}$$

3.3 Spin of Fock States and Spin-Singlet Fock States

We now pass from the d -electron sector to the full fermionic Fock space i.e., the direct sum of all particle-number sectors (see Section 2.1). The induced $\mathfrak{su}(2)$ -action preserves each particle sector $\mathcal{H}_k = \wedge^k \mathcal{H}$ and, in the canonical exterior basis, the action of element $g \in \mathfrak{su}(2)$ is represented by the block diagonal matrix

$$\hat{g} = g^{(0)} \oplus g^{(1)} \oplus \cdots \oplus g^{(2m)}, \quad (46)$$

where $g^{(\ell)}$ is defined in Eq. (20). We can now define the subspace $\mathcal{F}^{\text{SU}(2)} \subsetneq \mathcal{F}$ of total-spin singlet states as the direct sum of total-spin singlets in all particle sectors, i.e.,

$$\mathcal{F} = \bigoplus_{\ell=0}^{2m} \mathcal{H}_\ell, \quad \text{and} \quad \mathcal{F}^{\text{SU}(2)} = \bigoplus_{\ell=0}^{2m} \mathcal{H}_\ell^{\text{SU}(2)} = \bigoplus_{k=0}^m \mathcal{H}_{2k}^{\text{SU}(2)}. \quad (47)$$

Since $\mathcal{H}_\ell^{\text{SU}(2)} = \{0\}$ for odd ℓ , while $\dim(\mathcal{H}_{2k}^{\text{SU}(2)}) = N(m+1, k+1)$ for $0 \leq k \leq m$, the identity in Eq. (44) yields

$$\dim(\mathcal{F}^{\text{SU}(2)}) = \sum_{k=0}^m N(m+1, k+1) = C_{m+1}. \quad (48)$$

We recall that $\text{FD}_{2m} \cong \text{End}(\mathcal{F}) \cong \mathcal{F} \otimes \mathcal{F}^\dagger$, hence, we can write elements FD_{2m} as

$$\hat{\Omega} = \sum_{I, J \subseteq \llbracket m \rrbracket} a_{I, J} e_I \otimes e_J^\dagger. \quad (49)$$

Therefore, we can canonically induce an $\mathfrak{su}(2)$ -action on $\text{End}(\mathcal{F})$, via the action on \mathcal{F} and its conjugate \mathcal{F}^\dagger . This yields the following action for $\mathfrak{su}(2)$,

$$g(\hat{\Omega}) = \sum_{I, J \subseteq \llbracket m \rrbracket} a_{I, J} g(e_I) \otimes e_J^\dagger - \sum_{I, J \subseteq \llbracket m \rrbracket} a_{I, J} e_I \otimes g(e_J^\dagger) = \hat{g}\hat{\Omega} - \hat{\Omega}\hat{g} = [\hat{g}, \hat{\Omega}]. \quad (50)$$

Here \hat{g} is the $2^{2m} \times 2^{2m}$ matrix defined in Eq. (46). The operator \hat{g} is an endomorphism of \mathcal{F} and thus it is an element in the Fermi–Dirac algebra. The Fermi–Dirac representation of the generators S_\pm and S_z of $\mathfrak{su}(2)$ is

$$\hat{S}_+ = - \sum_{k=1}^m a_{k\uparrow}^\dagger a_{k\downarrow}, \quad \hat{S}_- = - \sum_{k=1}^m a_{k\downarrow}^\dagger a_{k\uparrow}, \quad \hat{S}_z = \frac{1}{2} \sum_{k=1}^m (a_{k\uparrow}^\dagger a_{k\uparrow} - a_{k\downarrow}^\dagger a_{k\downarrow}). \quad (51)$$

Note that the elements in the Fermi–Dirac algebra, FD_{2m} , that vanish under the $\mathfrak{su}(2)$ -action defined in Eq. (50) are precisely those that commute with \hat{S}_\pm and \hat{S}_z .

4 Spin-Adapted Coupled Cluster Theory

The (spin-free) electronic Hamiltonian in Eq. (9) is $\text{SU}(2)$ -invariant. This follows since it commutes with the generators of the induced $\mathfrak{su}(2)$ -action on Fock space. In symbols

$$[\hat{H}, \hat{S}_+] = [\hat{H}, \hat{S}_-] = [\hat{H}, \hat{S}_z] = 0. \quad (52)$$

Consequently, \hat{H} commutes with the Casimir operator \hat{S}^2 , and preserves the decomposition of the Hilbert space into $\text{SU}(2)$ -isotypic components. The *spin-singlet Schrödinger equation* can therefore be defined as the eigenvalue problem for $\text{SU}(2)$ -invariant quantum states,

$$\hat{H}\psi = E\psi, \quad \psi \in \mathcal{H}_d^{\text{SU}(2)}. \quad (53)$$

We recall that coupled cluster theory employs the ansatz

$$\psi = e^{\hat{T}} e_{[k]} \quad (54)$$

where *the cluster matrix* $\hat{T} \in \text{End}(\mathcal{F})$ is the new unknown and $e_{[k]} \in \mathcal{F}$ is the reference state [28, 81]. In particular, we choose the reference state as a closed-shell spin-restricted state (as in restricted Hartree-Fock theory).

Remark 4.1. The *closed-shell spin-restricted reference state*

$$\phi_0 = e_{[k]} = e_{1\downarrow} \wedge e_{1\uparrow} \wedge \cdots \wedge e_{k\downarrow} \wedge e_{k\uparrow}$$

is a singlet state. This can be seen by observing that it is annihilated by the generators \hat{S}_\pm and \hat{S}_z . Note that the \hat{S}_z -action vanishes by Remark 3.3. Moreover, the raising operator \hat{S}_+ acts by replacing a \downarrow -spin electron in a given orbital by an \uparrow -spin electron in the same orbital. Since the reference state is a closed shell state, it follows by Pauli's exclusion principle that $\hat{S}_+ e_{[k]} = 0$. The same argument holds for \hat{S}_- .

Since the reference state $e_{[k]}$ is a singlet, the physically relevant correlated ansätze may be taken entirely within the singlet sector. In other words, we can formulate the coupled cluster equations within the $\text{SU}(2)$ -invariant space of \mathcal{H}_d .

4.1 Spin Singlet Truncation Varieties

Coupled cluster theory is commonly formulated in the molecular orbital (particle-hole) picture [28]. Accordingly, we focus on the subalgebra of FD_{2m} generated by the occupied annihilators $\hat{a}_{i\alpha}$, $i \in [k]$, and the virtual creators $\hat{a}_{b\alpha}^\dagger$, $b \in [m] \setminus [k]$ (with $\alpha \in \{\uparrow, \downarrow\}$). These generators mutually anticommute, so this subalgebra is an exterior algebra. In symbols,

$$\mathbb{C}\langle \hat{a}_{1\downarrow}, \hat{a}_{1\uparrow}, \dots, \hat{a}_{k\downarrow}, \hat{a}_{k\uparrow}, \hat{a}_{k+1,\downarrow}^\dagger, \hat{a}_{k+1,\uparrow}^\dagger, \dots, \hat{a}_{m\downarrow}^\dagger, \hat{a}_{m\uparrow}^\dagger \rangle / \langle G \rangle \cong \wedge \mathbb{C}^{2m},$$

where G denotes the set of relations in Eq. (8). Since the electronic Hamiltonian conserves particle number, we restrict to the particle-number preserving subalgebra \mathcal{V} generated by the excitation words $\hat{a}_{b\alpha}^\dagger \hat{a}_{i\beta}$ of bidegree $(1, 1)$, where $i \in [k]$, $b \in [m] \setminus [k]$, and $\alpha, \beta \in \{\uparrow, \downarrow\}$. Since these generators are words of degree two in FD_{2m} , the induced product on \mathcal{V} is commutative, and hence \mathcal{V} is a commutative ring. It is also a graded ring graded by the excitation levels. Hence $\mathcal{V} = \bigoplus_{\ell=0}^d \mathcal{V}^{(\ell)}$, where the ℓ th grading $\mathcal{V}^{(\ell)}$ is a vector space generated by words with excitation level ℓ (degree ℓ monomials):

$$\hat{a}_{b_1,\alpha_1}^\dagger \hat{a}_{i_1\beta_1} \cdots \hat{a}_{b_\ell,\alpha_\ell}^\dagger \hat{a}_{i_\ell\beta_\ell} = \hat{a}_{b_\ell,\alpha_\ell}^\dagger \cdots \hat{a}_{b_1,\alpha_1}^\dagger \hat{a}_{i_1\beta_1} \cdots \hat{a}_{i_\ell\beta_\ell}.$$

By Pauli's exclusion principle ($(a_p^\dagger)^2 = 0$) it follows that $\mathcal{V}^{(d+1)} = \{0\}$. That is, the elements of \mathcal{V} are nilpotent of order at most d . Elements in \mathcal{V} can thus be written as sums of graded elements: $\hat{T} = \hat{T}_0 + \hat{T}_1 + \hat{T}_2 + \cdots + \hat{T}_d$ where

$$\hat{T}_\ell = \sum_{\substack{I \subseteq [k], B \subseteq [m] \setminus [k] \\ |I|=|B|=\ell}} t_{I,B} \hat{a}_{b_\ell,\alpha_\ell}^\dagger \cdots \hat{a}_{b_1,\alpha_1}^\dagger \hat{a}_{i_1\beta_1} \cdots \hat{a}_{i_\ell\beta_\ell} = \sum_{\substack{I \subseteq [k], B \subseteq [m] \setminus [k] \\ |I|=|B|=\ell}} t_{I,B} \hat{a}_B^\dagger \hat{a}_I \in \mathcal{V}^{(\ell)}.$$

The coordinates $t_{I,B} \in \mathbb{C}$ of \mathcal{V} are called *cluster amplitudes*. Note that the indexing sets $\llbracket m \rrbracket$ and $\llbracket k \rrbracket$ are of size $n = 2m$ and $d = 2k$ respectively and hence the combinatorial identity $\sum_{\ell=0}^d \binom{d}{\ell} \binom{n-d}{\ell} = \binom{n}{d}$ reveals that $\mathcal{V} \cong \mathbb{C}^{\binom{n}{d}}$.

Proposition 4.2. *With the induced $\mathfrak{su}(2)$ –actions on $\mathcal{H}_{2k} \subseteq \mathcal{F}$ and on \mathcal{V} (via $g \cdot \hat{T} = [\hat{g}, \hat{T}]$, cf. Eq. (50)), the map*

$$\Phi : \mathcal{V} \rightarrow \mathcal{H}_{2k}, \quad \hat{T} \mapsto \hat{T} e_{\llbracket k \rrbracket}. \quad (55)$$

is an isomorphism of $\mathfrak{su}(2)$ –modules.

Proof. The coordinates of $\Phi(\hat{T})$ are of the form $\hat{a}_B^\dagger \hat{a}_I e_{\llbracket k \rrbracket} = (-1)^\sigma e_J$, where $J = (\llbracket k \rrbracket \setminus I) \cup B$ and the sign σ is the sign of the permutation $\llbracket k \rrbracket \mapsto (I, J \cap \llbracket k \rrbracket)$. This proves Φ is a bijection. The reference state $e_{\llbracket k \rrbracket}$ is a closed-shell spin singlet by Remark 4.1. Therefore, for any $\hat{T} \in \mathcal{V}$ and any $g \in \mathfrak{su}(2)$ we get that

$$\Phi(g \cdot \hat{T}) = \Phi([\hat{g}, \hat{T}]) = [\hat{g}, \hat{T}] e_{\llbracket k \rrbracket} = \hat{g} \hat{T} e_{\llbracket k \rrbracket} - \hat{T} \hat{g} e_{\llbracket k \rrbracket} = \hat{g} \Phi(\hat{T}) = g \cdot \Phi(\hat{T}). \quad (56)$$

Hence Φ is $\mathfrak{su}(2)$ –equivariant, and therefore an isomorphism of $\mathfrak{su}(2)$ –modules. \square

The isomorphism above also induces a grading on \mathcal{H}_{2k} : we say a basis vector e_J of \mathcal{H}_{2k} has degree (or excitation level) $|J \setminus \llbracket k \rrbracket|$, and we denote the ℓ th grading of \mathcal{H}_{2k} by $\mathcal{H}_{2k}^{(\ell)}$. As a consequence of Proposition 4.2, we can study the irreducible decomposition of \mathcal{H}_d via the irreducible decomposition of \mathcal{V} . In particular:

Corollary 4.3. *The map Φ restricts to the invariant spaces of \mathcal{V} and \mathcal{H}_{2k} . Therefore*

$$\mathcal{H}_{2k}^{\text{SU}(2)} \cong \mathcal{V}^{\text{SU}(2)}.$$

We want to find a homogeneous basis for $\mathcal{V}^{\text{SU}(2)}$. This is possible since the generators in Eq. (51) are homogeneous, and hence the $\mathfrak{su}(2)$ –action preserves excitation levels. In particular, each basis element lives in a grading $\mathcal{V}^{(\ell)}$ for some $1 \leq \ell \leq m$. We start with the simplest generators of $\mathcal{V}^{\text{SU}(2)}$, namely those of excitation level 1. The *excitation operators* are the homogeneous elements of bidegree $(1, 1)$ given by:

$$\hat{X}_{i,b} = \hat{a}_{b\uparrow}^\dagger \hat{a}_{i\uparrow} + \hat{a}_{b\downarrow}^\dagger \hat{a}_{i\downarrow}, \quad 1 \leq i \leq k < b \leq n.$$

They are linearly independent and commute with \hat{S}_\pm and \hat{S}_z and are therefore generators of $\mathcal{V}^{\text{SU}(2)}$. The *excitation ring* is the graded ring

$$R = \mathbb{C}[\hat{X}_{1,k+1}, \hat{X}_{1,k+2}, \dots, \hat{X}_{1,n}, \hat{X}_{2,k+1}, \dots, \hat{X}_{k,n}] \subseteq \mathcal{V},$$

i.e., R is the subring of \mathcal{V} generated by the $k(m - k)$ excitation operators. Since R is generated by degree one elements in \mathcal{V} , it inherits the grading of \mathcal{V} and $R^{(\ell)} \subseteq \mathcal{V}^{(\ell)}$ for all $1 \leq \ell \leq m$. Since the variables $\hat{X}_{i,b}$ commute with \hat{S}_\pm and \hat{S}_z , every polynomial in R also commutes with them and therefore we obtain a stricter inclusion $R \subseteq \mathcal{V}^{\text{SU}(2)}$.

Theorem 4.4. *The invariant space $\mathcal{V}^{\text{SU}(2)}$ is an Artinian ring. The excitation ring R coincides with the invariant ring, that is $R = \mathcal{V}^{\text{SU}(2)}$.*

Proof. The ring \mathcal{V} is Artinian, and hence its invariant ring $\mathcal{V}^{\text{SU}(2)}$ is too. We notice that R is a subring of the ring S generated by level-one words $\hat{x}_{i,b,\alpha} := \hat{a}_{b\alpha}^\dagger \hat{a}_{i\alpha}$ where $1 \leq i \leq k < b \leq m$ and $\alpha \in \{\downarrow, \uparrow\}$. Note S is a proper subring of \mathcal{V} , since we restrict to products with a fixed spin. The ring S has $2k(m - k)$ variables and can implicitly be described as

$$S \cong \mathbb{C}[x_{1,k+1,\downarrow}, x_{1,k+1,\uparrow}, \dots, x_{k,m,\downarrow}, x_{k,m,\uparrow}] \Big/ \langle x_{i,a,\alpha} x_{j,b,\alpha} + x_{j,a,\alpha} x_{i,b,\alpha} \rangle.$$

The ring R is isomorphic to the subring of S generated by the $k(m - k)$ linear combinations $\hat{x}_{i,b} := \hat{x}_{i,b,\uparrow} + \hat{x}_{i,b,\downarrow} = \hat{X}_{i,b}$, where $1 \leq i \leq k \leq b \leq m$. They fulfill the degree-three relations

$$\sum_{\tau \in S_3} \hat{x}_{i,\tau(a)} \hat{x}_{j,\tau(b)} \hat{x}_{\ell,\tau(c)} = 0, \quad \text{where } i \leq j \leq \ell \text{ and } a \leq b \leq c. \quad (57)$$

Let I be the ideal generated by these relations and so $R \cong \mathbb{C}[x_{1,k+1}, \dots, x_{k,m}]/I$. In [82, Theorem 1.2], Sverrisdóttir, together with Price and Stelzer, prove that these relations form a Gröbner basis and that the number of standard monomials is $N(m + 1, k + 1)$. Therefore R is a vector space of dimension $N(m + 1, k + 1)$. On the other hand, by Corollary 4.3 and Theorem 3.6:

$$\dim \mathcal{V}^{\text{SU}(2)} = \dim \mathcal{H}_{2k}^{\text{SU}(2)} = N(m + 1, k + 1). \quad (58)$$

Hence, it follows the claim $R = \mathcal{V}^{\text{SU}(2)}$. \square

Remark 4.5 (Explicit generators of the invariance space). The standard monomials of R mentioned in the proof of Theorem 4.4 form the desired homogeneous basis for $\mathcal{V}^{\text{SU}(2)}$. We look at the 2nd grading of R , i.e., the space $R^{(2)}$ of homogeneous polynomials in R of degree 2. There are no linear relations among the $\binom{km - k^2 + 1}{2}$ degree two monomials. Therefore they are standard monomials of R and form a basis for $R^{(2)}$. Together with the unit 1 and the degree one generators $\hat{X}_{i,b}$, they yield a basis for the subspace of $\mathcal{V}^{\text{SU}(2)}$ consisting of elements of degree at most 2. Now consider the 3rd grading $R^{(3)}$. There are linear relations among the degree three monomials in $\hat{X}_{i,b}$, namely the generators in (57). Consequently, an explicit description of the standard monomials and hence the basis elements of excitation level ≥ 3 requires additional combinatorial tools; see [82]. Since we focus here on the CCD and CCSD formalisms, for which only invariants up to degree two are required, we do not pursue these higher-degree invariants further.

For $1 \leq \ell \leq k$ we define the ℓ th truncated cluster operator \hat{T}_ℓ to be a general element in the ℓ th grading of $\mathcal{V}^{\text{SU}(2)}$. We can write the truncated cluster operators \hat{T}_1 and \hat{T}_2 explicitly:

$$\hat{T}_1 = \sum_{(i,b)} t_{i,b} \hat{X}_{i,b}, \quad \hat{T}_2 = \sum_{(i,b) \leq (j,c)} t_{ij,bc} \hat{X}_{i,b} \hat{X}_{j,c}, \quad \text{where } t_{i,b}, t_{ij,bc} \in \mathbb{C}. \quad (59)$$

Here the pairs $(i, b) \in [k] \times [m] \setminus [k]$ are ordered lexicographically, and the condition $(i, b) \leq (j, c)$ avoids double counting of quadratic monomials. We then define the cluster operator \hat{T} as the sum of the truncated cluster operators, that is $\hat{T} = \hat{T}_1 + \hat{T}_2 + \dots + \hat{T}_k$. We notice that

\hat{T} is a general element in the invariant space $\mathcal{V}^{\text{SU}(2)}$ with a zero constant term. We denote the space of cluster operators as

$$\mathcal{V}^{\text{SU}(2)'} = \bigoplus_{\ell=1}^{2k} \mathcal{V}_{(\ell)}^{\text{SU}(2)}, \quad \text{with} \quad \mathcal{V}_{(\ell)}^{\text{SU}(2)} := \mathcal{V}^{\text{SU}(2)} \cap \mathcal{V}^{(\ell)}.$$

This is the space of $\text{SU}(2)$ -invariant operators in \mathcal{V} with a zero constant term. Equivalently this is the space of nilpotent operators in $\mathcal{V}^{\text{SU}(2)}$, that is those \hat{T} such that $\hat{T}^{2k+1} = 0$.

Proposition 4.6. *The spin-singlet exponential map*

$$\mathcal{V}^{\text{SU}(2)'} \rightarrow \mathcal{H}_{2k}^{\text{SU}(2)}, \quad \hat{T} \mapsto \exp(\hat{T}) e_{[k]}, \quad (60)$$

is an injective polynomial map. Its image coincides with the subspace

$$\{\psi \in \mathcal{H}_{2k}^{\text{SU}(2)} : e_{[k]}^T \psi = 1\} \subset \mathcal{H}_{2k}^{\text{SU}(2)}.$$

and the corresponding restriction is a bijection with a polynomial inverse.

Proof. Take a cluster operator $\hat{T} \in \mathcal{V}^{\text{SU}(2)'}.$ We recall that \hat{T} is nilpotent and therefore $\exp(\hat{T})e_{[k]}$ has polynomial entries. The operator $\exp(\hat{T})$ also commutes with the generators \hat{S}_\pm and \hat{S}_z so $\exp(\hat{T})e_{[k]} \in \mathcal{H}_{2k}^{\text{SU}(2)}$ and the map is well defined and polynomial. Since \hat{T} is nilpotent, the diagonal entries of $\exp(\hat{T})$ are 1 and so $e_{[k]}^T \exp(\hat{T})e_{[k]} = 1$. The bijectivity and the existence of a polynomial inverse follow from the same excitation-level induction as in [32, Proposition 2.4], applied within the invariant subspaces. \square

Fix a *level set* $\sigma \subseteq [d]$, specifying the allowed excitation levels. For instance, when employing CCS, CCD or CCSD, we set $\sigma = \{1\}, \{2\}, \{1, 2\}$, respectively. Let $\mathcal{V}_\sigma^{\text{SU}(2)}$ denote the subspace of $\mathcal{V}^{\text{SU}(2)}$ consisting of operators whose excitation level lies in σ . Explicitly:

$$\mathcal{V}_\sigma^{\text{SU}(2)} := \bigoplus_{\ell \in \sigma} \mathcal{V}_{(\ell)}^{\text{SU}(2)} \subseteq \mathcal{V}^{\text{SU}(2)'}.$$

The restriction of the spin-singlet exponential map, defined in Proposition 4.6, to this subspace is injective. We may further compose it with the projective embedding

$$\mathcal{H}_{2k}^{\text{SU}(2)} \hookrightarrow \mathbb{P}\mathcal{H}_{2k}^{\text{SU}(2)} \cong \mathbb{P}^{N(m+1, k+1)-1}.$$

Analogous to the truncation varieties in [32, 51] we define the *spin-singlet truncation variety* $V_\sigma^{\text{SU}(2)} \subseteq \mathbb{P}\mathcal{H}_{2k}^{\text{SU}(2)}$ to be the Zariski closure of the image of $\mathcal{V}_\sigma^{\text{SU}(2)}$ under this composed map. Hence, the spin-singlet truncation varieties are parameterized by restrictions of the spin-singlet exponential map. In this paper we focus on CCS, CCD and CCSD, where the elements of the subspaces $\mathcal{V}_\sigma^{\text{SU}(2)}$ are the truncated cluster operators \hat{T}_1 , \hat{T}_2 and $\hat{T}_1 + \hat{T}_2$ in Eq. (59). The corresponding truncation varieties are then parameterized by vectors:

$$\psi = \exp(\hat{T}_1)e_{[k]}, \quad \psi = \exp(\hat{T}_2)e_{[k]}, \quad \psi = \exp(\hat{T}_1 + \hat{T}_2)e_{[k]}.$$

Example 4.7 (CCS for $m = 4, k = 2$). The CCS cluster operator is of the form

$$\hat{T}_1 = t_{1,3}\hat{X}_{1,3} + t_{2,3}\hat{X}_{2,3} + t_{1,4}\hat{X}_{1,4} + t_{2,4}\hat{X}_{2,4}.$$

We recall from [32, Theorem 3.5] that the (spin-orbital) CCS truncation variety is the Grassmannian $\text{Gr}(4, 8) \subseteq \mathbb{P}^{69}$ in its Plücker embedding. To relate this to the spin-singlet truncation variety, we compose the spin-singlet CCS exponential map with the natural inclusion $\mathcal{H}_4^{\text{SU}(2)} \hookrightarrow \mathcal{H}_4 \cong \mathbb{C}^{70}$. This yields a parametrization $\mathbb{C}^4 \rightarrow \mathbb{P}\mathcal{H}_4 \cong \mathbb{P}^{69}$ of $V_{\{1\}}^{\text{SU}(2)}$ in the cluster amplitudes $(t_{1,3}, t_{2,3}, t_{1,4}, t_{2,4})$, given by the maximal minors of the 4×8 matrix

$$\begin{pmatrix} 1 & 0 & 0 & 0 & t_{1,3} & 0 & t_{1,4} & 0 \\ 0 & 1 & 0 & 0 & 0 & t_{1,3} & 0 & t_{1,4} \\ 0 & 0 & 1 & 0 & t_{2,3} & 0 & t_{2,4} & 0 \\ 0 & 0 & 0 & 1 & 0 & t_{2,3} & 0 & t_{2,4} \end{pmatrix}. \quad (62)$$

Here the rows are indexed by $\llbracket 2 \rrbracket$ and the columns by $\llbracket 4 \rrbracket$. We further project the image onto the 20 dimensional subspace $\mathbb{P}\text{Sym}_2(\wedge^2 \mathbb{C}^4)$ described in Remark 3.4. The resulting map is the quadratic Veronese embedding ν_2 of the Plücker embedding of $\text{Gr}(2, 4) \subseteq \mathbb{P}^5$. More precisely, on the standard affine chart $p_{12} = 1$, the Plücker coordinates are

$$(p_{12}, p_{13}, p_{23}, p_{14}, p_{24}, p_{34}) = (1, t_{2,3}, -t_{1,3}, t_{2,4}, -t_{1,4}, t_{1,3}t_{2,4} - t_{2,3}t_{1,4}).$$

Composing with ν_2 gives all degree two monomials in the Plücker coordinates. Consequently, the spin-singlet truncation variety embedded into $\mathbb{P}\text{Sym}_2(\wedge^2 \mathbb{C}^4)$ is the Veronese square of the Grassmannian:

$$V_{\{1\}}^{\text{SU}(2)} = \nu_2(\text{Gr}(2, 4)) \subseteq \mathbb{P}\text{Sym}^2(\wedge^2 \mathbb{C}^4).$$

In particular, $V_{\{1\}}^{\text{SU}(2)}$ has dimension 4 and degree 32. Notice that the ambient singlet space $\mathcal{H}_4^{\text{SU}(2)}$ has projective dimension 19, whereas $\text{Sym}^2(\wedge^2 \mathbb{C}^4)$ has projective dimension 20. The difference is accounted for by the Plücker relation

$$p_{12}p_{34} - p_{13}p_{24} + p_{23}p_{14} = 0,$$

which becomes a *linear* relation among the Veronese coordinates. We can therefore project onto $\mathbb{P}\mathcal{H}_4^{\text{SU}(2)}$ and embed the truncation variety $\nu_2(\text{Gr}(2, 4))$ into that space.

This example generalizes to arbitrary m and k :

Theorem 4.8. *The singlet CCS truncation variety is isomorphic to the Veronese square of the Grassmannian, specifically $V_{\{1\}}^{\text{SU}(2)} \cong \nu_2(\text{Gr}(k, m))$. In particular,*

$$\dim V_{\{1\}}^{\text{SU}(2)} = k(m - k), \quad \text{and} \quad \deg V_{\{1\}}^{\text{SU}(2)} = 2^{k(m-k)} \deg(\text{Gr}(k, m)). \quad (63)$$

Proof. Recall that the Plücker embedding parameterizes the Grassmannian $\text{Gr}(k, m)$ by the maximal minors of a $k \times m$ matrix $m(t) = (I_k \ t)$. Here $t = (t_{i,b})_{1 \leq i \leq k < b \leq m}$ is a $k \times (m - k)$ matrix with the CCS cluster amplitudes as entries. We denote the *Plücker coordinates* by $p_I(t) = \det(m(t)_I)$ where $I \subseteq [m]$ and $|I| = k$.

We consider the composition of the spin-singlet exponential map with the natural inclusion $\mathcal{H}_d^{\text{SU}(2)} \hookrightarrow \mathcal{H}_d \cong \mathbb{C}^{\binom{n}{d}}$. Its coordinates are the maximal minors of a $d \times n$ matrix $M(t)$, analogues to Eq. (62). The columns of this matrix are indexed by the spin orbitals, i.e., $\llbracket m \rrbracket$, and the rows by the occupied spin orbitals, i.e., $\llbracket k \rrbracket$. Row and column permutation such that spin-up orbitals precede spin-down orbitals yields a block-diagonalization of $M(t)$, i.e.

$$M'(t) = \begin{pmatrix} m(t) & 0_{k,m-k} \\ 0_{k,m-k} & m(t) \end{pmatrix}.$$

The maximal minors of $M'(t)$ can be computed using $k \times k$ Laplace expansion. First, we note that a $2k \times 2k$ minor of $M'(t)$ is nonzero only if it selects exactly k columns from the spin-down block and k columns from the spin-up block. Now for $I, J \in \binom{[m]}{k}$ we get

$$\det(M'(t)_{\{I\downarrow\} \cup \{J\uparrow\}}) = \det(m(t)_I) \det(m(t)_J) = p_I(t) p_J(t). \quad (64)$$

These are the coordinates of the composed map. We have now embedded the spin-singlet truncation variety into the full space of quantum state, and want to project down again to the space of $\text{SU}(2)$ -invariants. To that end, we embed the image into the space $\mathbb{P} \text{Sym}_2(\wedge^k \mathbb{C}^m)$ – as is described in Remark 3.4. We obtain the Veronese embedding of $\text{Gr}(k, m)$:

$$\mathbb{C}^{k \times (m-k)} \rightarrow \mathbb{P}^{\binom{m}{k}-1} \rightarrow \mathbb{P} \text{Sym}_2(\wedge^k \mathbb{C}^m), \quad t \mapsto (p_I(t) p_J(t))_{I \leq J \in \binom{[m]}{k}}.$$

By Proposition 4.6 the spin-singlet exponential parameterization maps into the invariant space $\mathcal{H}_{2k}^{\text{SU}(2)}$, so we can further embed the Veronese square of the Grassmannian into $\mathbb{P} \mathcal{H}_{2k}^{\text{SU}(2)}$. Note that there are linear relations among the coordinates, namely, the Plücker relations – quadratic equations in the $p_I(t)$ that cut out the Grassmannian. There are exactly

$$\dim(\text{Sym}_2(\wedge^k \mathbb{C}^m)) - \dim(\mathcal{H}_{2k}^{\text{SU}(2)}) = \binom{\binom{m}{k} + 1}{2} - N(m+1, k+1).$$

Plücker relations, minimally generating the Grassmannian. The projection of the Veronese square into $\mathbb{P} \mathcal{H}_{2k}^{\text{SU}(2)}$ is therefore also an embedding of $\nu_2(\text{Gr}(k, m))$. \square

We notice the Grassmannian of lines in m -dimensional space is a projective space, namely $\text{Gr}(1, m) \cong \mathbb{P}^{m-1}$, and therefore linear. The CCS spin-singlet truncation varieties corresponding to one electron pair, $k = 1$, are therefore the *2nd Veronese varieties*, $V_{\{1\}}^{\text{SU}(2)} \cong \nu_2(\mathbb{P}^{m-1})$.

4.2 Spin-Adapted Coupled Cluster Equations

The truncation varieties are used to approximate the solutions of the Schrödinger equation Eq. (53). We fix a level set σ and consider the spin-singlet truncation variety $V_{\sigma}^{\text{SU}(2)}$. In general, none of the quantum states on $V_{\sigma}^{\text{SU}(2)}$ will be eigenvectors of the Hamiltonian. We then relax the constraints of the eigenvalue problem and define the coupled cluster equations:

$$(\hat{H}\psi)_{\sigma} = E\psi_{\sigma}, \quad \psi \in V_{\sigma}^{\text{SU}(2)}. \quad (65)$$

Here ψ_σ denotes the projection of quantum state ψ onto coordinates ψ_I with excitation level $|I \setminus [k]| \in \sigma$. Hence, $(\cdot)_\sigma$ defines a projection from \mathcal{H}_{2k} onto the graded subspace $\bigoplus_{\ell \in \sigma} \mathcal{H}_{2k}^{(\ell)}$.

For generic parameters h_{pq} and v_{pqrs} , the number of solutions to the CC equations in Eq. (65) is finite and fixed. We call this number the *coupled cluster degree* of the truncation variety $V_\sigma^{\text{SU}(2)}$ and denote it by $\text{CCdeg}(V_\sigma^{\text{SU}(2)})$. By the parameter continuation theorem [83, Theorem 1], the CC degree serves as an upper bound to the number of solutions of Eq. (65) for any Hamiltonian operator \hat{H} . Computing the CC degree of a truncation variety is generally difficult, as it requires solving the CC equations for a generic Hamiltonian \hat{H} . Nevertheless, one can obtain an upper bound in terms of invariants of $V_\sigma^{\text{SU}(2)}$:

Proposition 4.9. *The coupled cluster degree of $V_\sigma^{\text{SU}(2)}$ fulfills the following inequality:*

$$\text{CCdeg}(V_\sigma^{\text{SU}(2)}) \leq (\dim(V_\sigma^{\text{SU}(2)}) + 1) \deg(V_\sigma^{\text{SU}(2)}).$$

The proof of this Proposition is omitted as it is analogous to the proof of [32, Theorem 5.2]. The dimension of a truncation variety can easily be computed by counting basis vectors with excitation level in σ . For example, the CCS and CCD spin-singlet truncation varieties have the dimensions

$$\dim(V_{\{1\}}^{\text{SU}(2)}) = k(m - k), \quad \dim(V_{\{2\}}^{\text{SU}(2)}) = \binom{k(m - k) + 1}{2},$$

respectively, and the dimension of the CCSD truncation variety is their sum. Finding an explicit formula for the degree of a truncation variety is more challenging. In the CCS case, an explicit formula was obtained in Theorem 4.8. By contrast, for CCD and CCSD no such formula is known, and the degree for specific values of k and m must be determined numerically. In some cases, we can obtain explicit formulas for the CC degree itself, such as:

Theorem 4.10. *Let $k = 1$. The CC degree of the 2nd Veronese variety $V_{\{1\}}^{\text{SU}(2)} \cong \nu_2(\mathbb{P}^{m-1})$ is*

$$\text{CCdeg}(\nu_2(\mathbb{P}^{m-1})) = 2^m - 1.$$

The CC and ED degrees of the Veronese variety coincide, see [84].

Proof. Here $k = 1$ and so the dimension of the invariant space simplifies to

$$\dim(\mathcal{H}_{2k}^{\text{SU}(2)}) = N(m + 1, 2) = \binom{m + 1}{2}.$$

Remark 3.4 implies that, in this case, $\mathcal{H}_2^{\text{SU}(2)} \cong \text{Sym}_2(\mathbb{C}^m)$, so the basis vectors of $\mathcal{H}_2^{\text{SU}(2)}$ are $e_{i\downarrow, i\uparrow}$ and $e_{i\downarrow, j\uparrow} + e_{i\uparrow, j\downarrow}$. They are indexed by subsets in $[m]$ of size one and two. Also, the Veronese square $x^{\otimes 2} \in \nu_2(\mathbb{P}^{m-1})$ of $x \in \mathbb{P}^{m-1}$ projects onto x under truncation, that is $(x^{\otimes 2})_{\{1\}} = x$. We can therefore rewrite the CC equations as

$$H_{\{1\}} x^{\otimes 2} = Ex, \quad x \in \mathbb{P}^{m-1}, \tag{66}$$

where $H_{\{1\}}$ is a $m \times \binom{m+1}{2}$ submatrix of the generic Hamiltonian \hat{H} , with only the rows indexed by singletons in $[m]$. We can construct a generic $m \times m \times m$ symmetric tensor η such

that $H_{\{1\}}$ has entries $H_{i,j\ell} = \eta_{i,j}\eta_{i,\ell}$. The tensor η uniquely corresponds to a homogeneous polynomial of degree three, given by $F_\eta = \langle \eta, x^{\otimes 3} \rangle$, and its gradient satisfies $\nabla F_\eta = H_{\{1\}}x^{\otimes 2}$. The CC equations in Eq. (66) are therefore precisely the fixed-point equations of ∇F_h . Equivalently, they are the eigenpair equations for the symmetric tensor η . Since \hat{H} and η are generic tensors we get by [84, Theorem 12.17] that the CC degree is $2^m - 1$. \square

In Eq. (65) we formulate the unlinked coupled cluster equations in an algebraic way. This might be unintuitive for readers that are experienced in electronic structure theory. Nonetheless this formulation is important to prove results such as Proposition 4.9. However, this presentation is not optimal for explicitly solving the CC equations. Since the restriction of the exponential map to \mathcal{V}_σ is injective, we can write the unlinked coupled cluster equations in the following way:

$$((\hat{H} - E \cdot \hat{I}_\mathcal{F}) \exp(\hat{T}_\sigma) e_{[k]})_\sigma = 0. \quad (67)$$

This is a square polynomial system of size $\dim(V_\sigma^{\text{SU}(2)}) + 1$, whose variables are the energy E and the cluster amplitudes $t_{I,B}$ with excitation level $|I| \in \sigma$. Using this formulation, we can solve the CC equations with `HomotopyContinuation.jl` [85]. For an in-depth description on how to solve the coupled cluster equations, we refer the reader to [33].

We close this chapter with a short remark on Löwdin's symmetry dilemma:

Remark 4.11. Although the Hamiltonian is $\text{SU}(2)$ -invariant and its exact eigenstates can be chosen as simultaneous eigenstates of \hat{S}^2 and \hat{S}_z , approximate ansätze may face a trade-off commonly referred to as *Löwdin's symmetry dilemma*. At the mean-field level, enforcing spin symmetry (e.g. restricted Hartree–Fock) yields a spin-pure reference but may give qualitatively poor energies in regimes of strong (static) correlation (for instance, along bond dissociation), because a single symmetry-adapted determinant cannot represent near-degeneracy effects. Allowing symmetry breaking (e.g. unrestricted Hartree–Fock) often lowers the energy and captures part of the static correlation, but produces *spin-contaminated* states that do not lie in $\mathcal{H}_d^{\text{SU}(2)}$. The same tension can propagate to correlated methods built on a mean-field reference. In *restricted* coupled cluster theory we deliberately formulate the equations on the $\text{SU}(2)$ -invariant sector, see Eq. (53), so that the CC state is spin-adapted by construction; however, this restriction can necessitate higher excitation rank to recover correlation effects that a broken-symmetry reference may mimic at lower rank. Alternative strategies include symmetry restoration (spin projection) applied to broken-symmetry references, which aims to combine the energetic flexibility of symmetry breaking with a final spin-pure wavefunction.

5 Numerical Simulations

A practical algebraic measure of computational complexity in CC theory is the *number of isolated solutions* (counted with multiplicity) for a generic instance of the CC equations, i.e., the *CC degree*. In homotopy-based solvers, the CC degree directly controls the number of solution paths that *must* be tracked, and is therefore a reliable proxy for runtime and memory. The central numerical message of this section is that imposing $\text{SU}(2)$ -spin adaptation reduces the CC degree by orders of magnitude, making exhaustive solution and continuation computations feasible in regimes where the spin-generalized formulation becomes

intractable. The simulations presented here were performed using the software packages `HomotopyContinuation.jl` [85] and `PySCF` [86–88].

5.1 Scaling of Generic Spin Restricted Systems

We begin by comparing the number of roots of the spin restricted coupled cluster equations with the number of roots of the spin generalized coupled cluster equations from [32, Section 5]. For $k = 1$ (and $d = 2$) we investigate how the CC degree scales with the number of spin orbitals n , both for the CC equations for singles ($\sigma = \{1\}$) and for doubles ($\sigma = \{2\}$), similar to [32, Example 6.3]. In Figure 1, the blue curve shows the spin-generalized CC degree (see Theorem 5.5 and Corollary 5.3 in [32] for CCS and CCD, respectively), while the orange curve shows the corresponding spin-restricted CC degree.

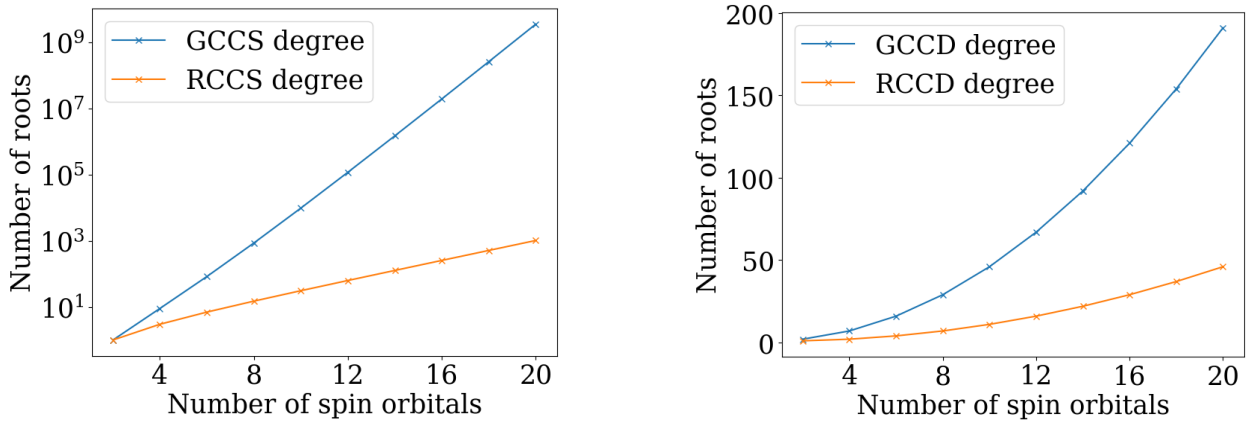


Figure 1: Comparison of the number of roots between spin restricted and spin generalized CC equations for CCS (left) and CCD (right) at $k = 1$. The reduction in degree translates into a corresponding reduction in the number of solution paths that must be tracked.

Figure 1 quantifies the reduction in generic solution complexity obtained by imposing $SU(2)$ -symmetry. For $k = 1$ and CCS, the spin-generalized degree grows to $\sim 10^9$ at 20 spin orbitals, whereas the spin-restricted degree is only $\sim 10^3$, corresponding to a reduction of roughly six orders of magnitude in the number of isolated solutions (and hence in the number of continuation paths in homotopy-based solvers). For CCD the degrees are smaller but the same trend persists: at 20 spin orbitals the degree decreases from about 190 (generalized) to about 45 (restricted), a reduction by a factor of ≈ 4 . These data indicate that spin adaptation yields a substantial algorithmic simplification of the CC polynomial systems already in the minimal-electron setting, motivating its use in the numerical studies below.

Indeed, we observe that the effect becomes numerically pronounced and computationally observable already for systems as small as four electrons. We compare CCD degrees for the spin-restricted and spin-generalized formalisms when $d = 4$ (two electron pairs, $k = 2$) and the number of spin-orbitals is $n = 8, 9, 10, 11, 12$. The spin-generalized CCD degrees are taken from [32, Section 5] where available, and for larger n we report the best available upper bounds from [89]. The resulting degrees are summarized in Table 1.

n	8	9	10	11	12
RCCD	20	–	998	–	$\sim 1.19 \cdot 10^7$
GCCD	72	1,823	2,523,135	$\leq 3.2 \cdot 10^{11}$	$\leq 1.18 \cdot 10^{23}$

Table 1: RCCD and GCCD degrees for four electrons ($d = 4$). For $n = 11, 12$ the GCCD entries are upper bounds. The collapse in degree under spin adaptation directly reflects a collapse in the number of solution branches.

Two features are noteworthy. First, even at modest size ($n = 10$), the degree collapses from 2,523,135 in GCCD to 998 in RCCD, a reduction by more than three orders of magnitude. Second, the available bounds indicate that the gap continues to widen rapidly as n grows, underscoring that spin adaptation is not a cosmetic symmetry constraint but a decisive computational simplification. We now illustrate how the incorporation of spin-adaptation pushes the boundaries of algebro computational exploration for chemical systems.

5.2 Lithium Hydride

Lithium hydride (LiH) has served as a small yet “chemically realistic” benchmark system for algebraic–computational studies. In a minimal-basis (STO-6G) description, LiH is modeled with four electrons (two electron pairs) in six spatial orbitals, i.e., twelve spin orbitals. The minimal spatial basis is given by the atomic orbitals

$$\text{H } 1s, \quad \text{Li } 1s, \quad \text{Li } 2s, \quad \text{Li } 2p_x, \quad \text{Li } 2p_y, \quad \text{Li } 2p_z.$$

Moreover, LiH exhibits a clear energetic separation between core and valence orbitals, as reflected in the molecular-orbital energies obtained from spin-restricted Hartree–Fock calculations [90]

$$(-2.51132217, -0.3024674, 0.06426691, 0.14495239, 0.14495239, 0.59035732).$$

The large gap to the lowest orbital is consistent with a chemically inert core, suggesting that LiH is well described by an active-space picture in which correlation is dominated by the valence pair, while core excitations are energetically suppressed. In the frozen core approximation we expect CCSD to be exact since this corresponds to a two-electron problem.

5.2.1 LiH Dissociation in a σ -Active Space

We may choose the Li–H bond axis as the z -axis of the coordinate frame. In this setting the electronic structure separates into σ and π symmetry subspaces: the $\text{Li } 2p_x$ and $\text{Li } 2p_y$ atomic orbitals transform as π functions (perpendicular to the bond) and therefore do not mix with the σ manifold that governs bonding. Consequently, the molecular-orbital coefficient matrix is block diagonal, with a decoupled $\{2p_x, 2p_y\}$ block. We therefore restrict our simulations to the σ -active space spanned by $\text{H } 1s$, $\text{Li } 1s$, $\text{Li } 2s$, and $\text{Li } 2p_z$, which yields an effective model with two electron pairs and four spatial orbitals. Note that if the linear symmetry were broken along the reaction path, this decoupling would no longer be exact and small σ – π

mixing could occur. Numerically, this decoupling is directly evident in the molecular-orbital (MO) coefficient matrix C from spin-restricted Hartree–Fock calculations [90] (exemplified at the LiH-equilibrium geometry):

$$C = \left[\begin{array}{ccc|cc|c} 0.974 & -0.328 & -0.147 & 0 & 0 & -0.385 \\ -0.009 & 0.370 & 0.881 & 0 & 0 & -0.952 \\ -0.020 & 0.441 & -0.548 & 0 & 0 & -1.076 \\ \hline 0 & 0 & 0 & 0 & 1 & 0 \\ 0 & 0 & 0 & 1 & 0 & 0 \\ \hline 0.072 & 0.535 & -0.183 & 0 & 0 & 1.557 \end{array} \right],$$

where two of the orbitals are supported entirely on the $\{\text{Li } 2p_x, \text{Li } 2p_y\}$ basis functions and have zero coefficients on the remaining atomic orbitals. Hence, C can indeed be arranged into a block diagonal matrix with a decoupled $2 \times 2 \pi$ -block. We investigate the root structure for RCCSD while dissociating LiH over bond lengths from 1 to 3 bohr. The spin-singlet CC degree in this case is

$$\text{CCdeg}(V_{\{1,2\}}^{\text{SU}(2)}) = 620.$$

opposed to the spin-generalized CC degree reported in [33]:

$$\text{CCdeg}(V_{\{1,2\}}) \approx 16,952,996.$$

We discretize the interval using an equidistant grid with 50 points and compute between 618 and 620 RCCSD solutions per grid point. For comparison, diagonalizing the corresponding Hamiltonian (i.e., a 20×20 real-valued symmetric matrix) yields 20 distinct eigenvalues.

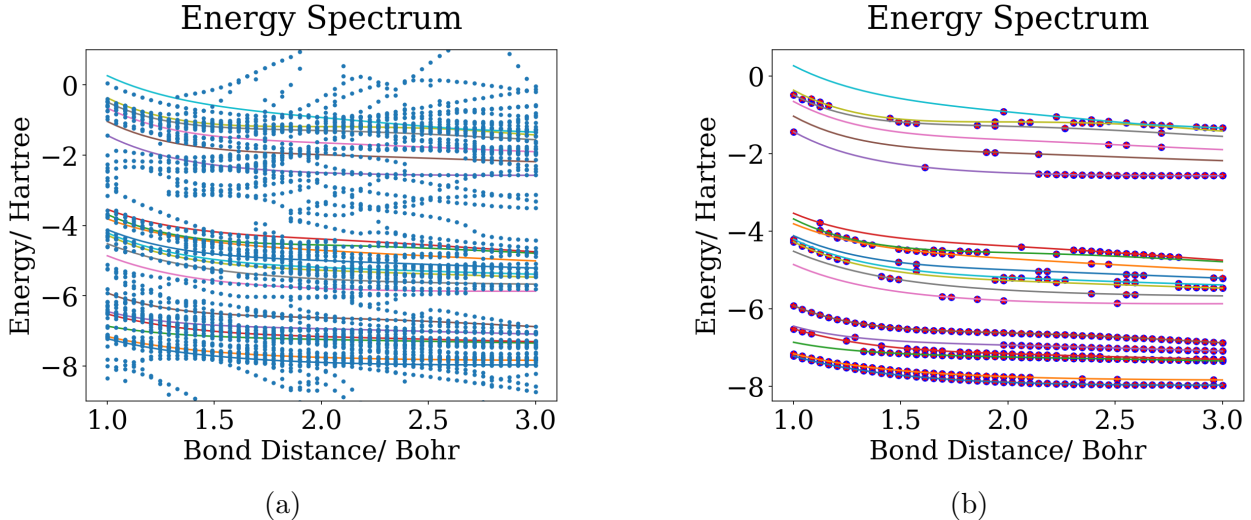


Figure 2: LiH dissociation in a minimal basis ($k = 2, m = 4$): comparison of RCCSD solution branches with the exact eigenvalue curves. (a) All RCCSD solution branches compared to the exact spectrum. (b) RCCSD solutions lying near an eigenvalue (the physically relevant).

Figure 2a shows all RCCSD solution branches together with the exact eigenvalue curves, while Figure 2b highlights only those RCCSD solutions that lie close to an eigenvalue, i.e., an energy difference of less than 10^{-3} .

5.3 All-electron LiH calculations

In previous algebro-computational investigations, all-orbital simulations for LiH were out of computational reach due to the sheer size of the CC polynomial system and the corresponding solution count. As reported in [32], the corresponding CCD and CCSD systems consist of 168 and 200 equations, respectively – well beyond the practical limits of current algebraic numerical solvers. Moreover, the number of homotopy paths that would need to be tracked vastly exceeds the approximately 1.7×10^7 paths tracked in [33], where the CCSD calculations for LiH in 8 spatial orbitals took over 30 days. In the present setting, however, imposing spin adaptation reduces the effective algebraic complexity sufficiently to make a RCCD solution-landscape computation feasible, for the all-electron system.

All subsequent computations were done on the MPI–MiS computer server, using four 18-Core Intel Xeon E7-8867 v4 at 2.4 GHz (3072 GB RAM). For the generic (random-coefficient) instance of the all-electron RCCD system, the monodromy solver required 21 days to recover the complete solution set, revealing the RCCD degree for $k = 2$ and $m = 6$ to be

$$\text{CCdeg}(V_{\{1,2\}}^{\text{SU}(2)}) \approx 11,920,113 \quad (68)$$

Recall that a lower bound for the same system in GCCD is 10^{23} , see Table 1. Once the generic solutions were obtained, a parameter homotopy tracked them to the LiH instances in 3 days and 48 minutes. This computation produced 67,909 solutions, of which 552 are non-singular and 106 are real. In Figure 3a we compare the full solution spectrum with the 71 distinct eigenvalues of the symmetric 105×105 Hamiltonian matrix. In Figure 3b we highlight the only those RCCD solutions that lie within a 10^{-3} radius of an eigenvalue. In total, this provides (to our knowledge) the first all-electron LiH computation in which the *entire* RCCD solution set is explicitly resolved.

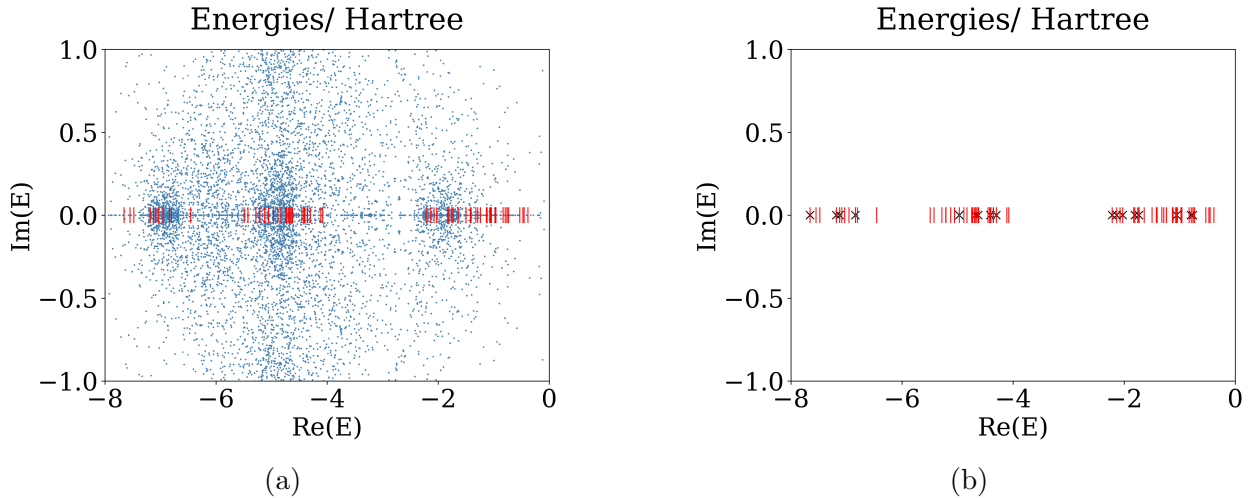


Figure 3: LiH dissociation in a full basis ($k = 2$, $m = 6$): comparison of RCCD solutions with the exact eigenvalues. (a) All RCCD solutions compared to the exact spectrum. (b) RCCD solutions lying near an eigenvalue (physically relevant).

The resulting all-electron picture reinforces two qualitative observations already present in the σ -active-space study. First, there are multiple physically relevant RCCD solutions close to exact eigenvalues. Second, the RCCD polynomial system admits additional, non-physical branches whose energies do not correspond to any eigenvalue of the Hamiltonian and may even fall below the exact ground-state energy. Such “overcorrelated” solutions are consistent with the non-variational character of coupled cluster theory, but here they appear as a *structural* feature of the RCCD algebraic solution set rather than a numerical accident. Their systematic presence in the all-electron calculation emphasizes the value of global solution methods (monodromy/parameter homotopy) for characterizing the full CC landscape and motivates *a posteriori* diagnostics for identifying the physically meaningful root among many mathematically valid ones [91–94].

5.4 Water

Water (H_2O) in a minimal basis set discretization has ten electrons (five electron pairs) in seven spatial orbitals, i.e., 14 spin orbitals. The minimal spatial basis is given by the atomic orbitals

$$\text{H } 1s, \quad \text{H } 1s, \quad \text{O } 1s, \quad \text{O } 2s, \quad \text{O } 2p_x, \quad \text{O } 2p_y, \quad \text{O } 2p_z.$$

We note that water exhibits a clear energetic separation between the core and valence manifolds at the Hartree–Fock level. The MO energies (in E_h) are

$$(-20.5043, -1.2759, -0.6209, -0.4593, -0.3975, 0.5970, 0.7299).$$

showing a large gap of $\Delta\varepsilon \approx 19.23 E_h$ (≈ 523 eV) between the lowest orbital and the remaining valence/virtual spectrum. This separation is consistent with a chemically inert core orbital, so that electron correlation relevant to bonding and low-energy excitations is dominated by the valence space, while core excitations are energetically suppressed.

To quantify the core character, we compute a Mulliken-like gross population of molecular orbital i on the chosen core atomic-orbital (AO) subspace [95, 96],

$$w_{\text{core}}^{(i)} = \sum_{\mu \in \text{core}} C_{\mu i} (SC)_{\mu i},$$

where C is the MO coefficient matrix and S is the AO overlap matrix. Taking the core subspace to be the oxygen $1s$ AO(s), we obtain for the lowest MO

$$w_{\text{O } 1s}^{(0)} = 0.996559,$$

indicating that MO 0 is essentially a pure $\text{O } 1s$ core orbital. We therefore adopt a frozen-core treatment by keeping this doubly occupied orbital inactive and correlating only the remaining (valence) orbitals. In practice, this corresponds to freezing MO 0 (the $\text{O } 1s$ orbital) in all post-HF and active-space calculations reported here.

We solved a generic instance of the RCCD equations for $k = 4$ and $m = 6$ using a monodromy solver. After running the solver for 6 days and 15 hours, we obtained 11,920,154

solutions. By particle–hole symmetry, the corresponding RCCD degree coincides with that for $k = 2$ and $m = 6$. Comparing this count with the approximate CC degree reported in Eq. (68), we find a discrepancy of 41 solutions. We attribute this discrepancy to numerical error and assume that both monodromy computations failed to detect some solutions. In [33, Monodromy], we describe the stopping criteria used in monodromy computations and explain why, by their very nature, such methods make it difficult to verify solution completeness. Consequently, the computed solution counts provide numerical approximations to the CC degree that are always lower bounds, and which with high probability are exact or very close to the true value. Once the generic solutions were obtained, a parameter homotopy tracked them to the H_2O instances in 13 hours, finding 10,628,368 solutions, of which 603 are singular and 7,396 are real. In Figure 4a we compare the full solution spectrum with the 105 distinct eigenvalues the nonsingular Hamiltonian matrix. In Figure 4b we highlight the only those RCCD solutions that lie within a 10^{-3} radius of an eigenvalue.

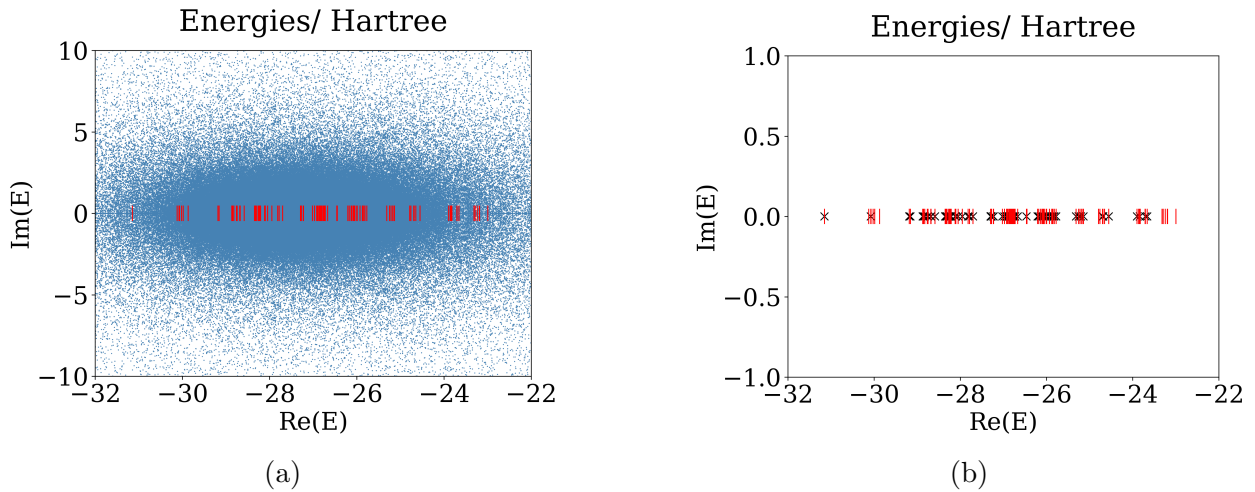


Figure 4: H_2O dissociation in a minimal basis ($k = 4, m = 6$): comparison of RCCD solutions with the exact eigenvalues. (a) All RCCD solutions compared to the exact spectrum. (b) RCCD solutions lying near an eigenvalue (physically relevant).

The full RCCD solution spectrum for H_2O appears as a cloud surrounding the exact eigenvalues, becoming denser toward the center of the spectrum. Consequently, some solution energies may lie close to an eigenvalue for purely statistical reasons, rather than reflecting physical significance. This indicates that further investigation into the numerical stability of the computed roots is needed. However, this lies beyond the scope of this manuscript and is left for future work.

Acknowledgment: We thank Veronica Calvo Cortes for her helpful insights on representation theory.

References

- [1] Tong Wang, Xinheng He, Mingyu Li, Yatao Li, Ran Bi, Yusong Wang, Chaoran Cheng, Xiangzhen Shen, Jiawei Meng, He Zhang, et al. Ab initio characterization of protein molecular dynamics with AI2BMD. *Nature*, 635(8040):1019–1027, 2024.
- [2] Naoya Aizawa, Yong-Jin Pu, Yu Harabuchi, Atsuko Nihonyanagi, Ryotaro Ibuka, Hiroyuki Inuzuka, Barun Dhara, Yuki Koyama, Ken-ichi Nakayama, Satoshi Maeda, et al. Delayed fluorescence from inverted singlet and triplet excited states. *Nature*, 609(7927):502–506, 2022.
- [3] James Kirkpatrick, Brendan McMorrow, David HP Turban, Alexander L Gaunt, James S Spencer, Alexander GDG Matthews, Annette Obika, Louis Thiry, Meire Fortunato, David Pfau, et al. Pushing the frontiers of density functionals by solving the fractional electron problem. *Science*, 374(6573):1385–1389, 2021.
- [4] Zhi-Hao Cui, Huachen Zhai, Xing Zhang, and Garnet Kin-Lic Chan. Systematic electronic structure in the cuprate parent state from quantum many-body simulations. *Science*, 377(6611):1192–1198, 2022.
- [5] Yueqing Chang, Erik GCP van Loon, Brandon Eskridge, Brian Busemeyer, Miguel A Morales, Cyrus E Dreyer, Andrew J Millis, Shiwei Zhang, Tim O Wehling, Lucas K Wagner, et al. Downfolding from ab initio to interacting model Hamiltonians: comprehensive analysis and benchmarking of the DFT+ cRPA approach. *npj Computational Materials*, 10(1):129, 2024.
- [6] Basile Herzog, Alejandro Gallo, Felix Hummel, Michael Badawi, Tomáš Bučko, Sébastien Lebègue, Andreas Grüneis, and Dario Rocca. Coupled cluster finite temperature simulations of periodic materials via machine learning. *npj Computational Materials*, 10(1):68, 2024.
- [7] Masaya Hagai, Naoto Inai, Takuma Yasuda, Kazuhiro J Fujimoto, and Takeshi Yanai. Extended theoretical modeling of reverse intersystem crossing for thermally activated delayed fluorescence materials. *Science Advances*, 10(5):eadk3219, 2024.
- [8] Yan-Yun Jing, Nengquan Li, Xiaosong Cao, Han Wu, Jingsheng Miao, Zhanxiang Chen, Manli Huang, Xinzhang Wang, Yuxuan Hu, Yang Zou, et al. Precise modulation of multiple resonance emitters toward efficient electroluminescence with pure-red gamut for high-definition displays. *Science Advances*, 9(30):eadh8296, 2023.
- [9] Benjamin X Shi, Andrew S Rosen, Tobias Schäfer, Andreas Grüneis, Venkat Kapil, Andrea Zen, and Angelos Michaelides. An accurate and efficient framework for modelling the surface chemistry of ionic materials. *Nature chemistry*, 17(11):1688–1695, 2025.
- [10] Rodney J Bartlett and Monika Musiał. Coupled-cluster theory in quantum chemistry. *Reviews of Modern Physics*, 79(1):291, 2007.

- [11] T Daniel Crawford and Henry F Schaefer III. An introduction to coupled cluster theory for computational chemists. *Reviews in computational chemistry*, 14:33–136, 2007.
- [12] Hermann Kümmel. Origins of the coupled cluster method. *Theoretica Chimica Acta*, 80(2-3):81–89, 1991.
- [13] Jiří Čížek. Origins of coupled cluster technique for atoms and molecules. *Theoretica Chimica Acta*, 80(2-3):91–94, 1991.
- [14] R.J. Bartlett. How and why coupled-cluster theory became the preeminent method in ab initio quantum chemistry. In C. Dykstra, G. Frenking, K. Kim, and G. Scuseria, editors, *Theory and Applications of Computational Chemistry (The First Forty Years)*, pages 1191–1221. 1st edition edition, 2005.
- [15] Josef Paldus. The beginnings of coupled cluster theory: An eyewitness account. In C. Dykstra, G. Frenking, K. Kim, and G. Scuseria, editors, *Theory and Applications of Computational Chemistry (The First Forty Years)*, pages 115–147. 1st edition, 2005.
- [16] Jouko S Arponen. Independent-cluster methods as mappings of quantum theory into classical mechanics. *Theoretica Chimica Acta*, 80(2-3):149–179, 1991.
- [17] RF Bishop. An overview of coupled cluster theory and its applications in physics. *Theoretica Chimica Acta*, 80(2-3):95–148, 1991.
- [18] Lucie Gráfová, Michal Pitonak, Jan Rezac, and Pavel Hobza. Comparative study of selected wave function and density functional methods for noncovalent interaction energy calculations using the extended S22 data set. *Journal of chemical theory and computation*, 6(8):2365–2376, 2010.
- [19] Tait Takatani, Edward G Hohenstein, Massimo Malagoli, Michael S Marshall, and C David Sherrill. Basis set consistent revision of the S22 test set of noncovalent interaction energies. *The Journal of chemical physics*, 132(14), 2010.
- [20] Petr Jurečka, Jiří Šponer, Jiří Černý, and Pavel Hobza. Benchmark database of accurate (MP2 and CCSD (T) complete basis set limit) interaction energies of small model complexes, DNA base pairs, and amino acid pairs. *Physical Chemistry Chemical Physics*, 8(17):1985–1993, 2006.
- [21] Jan Rezáć, Kevin E Riley, and Pavel Hobza. S66: A well-balanced database of benchmark interaction energies relevant to biomolecular structures. *Journal of chemical theory and computation*, 7(8):2427–2438, 2011.
- [22] Jan Rezac, Kevin E Riley, and Pavel Hobza. Benchmark calculations of noncovalent interactions of halogenated molecules. *Journal of chemical theory and computation*, 8(11):4285–4292, 2012.

- [23] Raghunathan Ramakrishnan, Pavlo O Dral, Matthias Rupp, and O Anatole Von Lilienfeld. Big data meets quantum chemistry approximations: the δ -machine learning approach. *Journal of chemical theory and computation*, 11(5):2087–2096, 2015.
- [24] Justin S Smith, Benjamin T Nebgen, Roman Zubatyuk, Nicholas Lubbers, Christian Devereux, Kipton Barros, Sergei Tretiak, Olexandr Isayev, and Adrian E Roitberg. Approaching coupled cluster accuracy with a general-purpose neural network potential through transfer learning. *Nature communications*, 10(1):2903, 2019.
- [25] Justin S Smith, Roman Zubatyuk, Benjamin Nebgen, Nicholas Lubbers, Kipton Barros, Adrian E Roitberg, Olexandr Isayev, and Sergei Tretiak. The ANI-1ccx and ANI-1x data sets, coupled-cluster and density functional theory properties for molecules. *Scientific data*, 7(1):134, 2020.
- [26] Marcel Ruth, Dennis Gerbig, and Peter R Schreiner. Machine learning of coupled cluster (t)-energy corrections via delta (δ)-learning. *Journal of Chemical Theory and Computation*, 18(8):4846–4855, 2022.
- [27] János Daru, Harald Forbert, Jörg Behler, and Dominik Marx. Coupled cluster molecular dynamics of condensed phase systems enabled by machine learning potentials: Liquid water benchmark. *Physical Review Letters*, 129(22):226001, 2022.
- [28] Jiří Čížek. On the correlation problem in atomic and molecular systems. calculation of wavefunction components in ursell-type expansion using quantum-field theoretical methods. *The Journal of Chemical Physics*, 45(11):4256–4266, 1966.
- [29] George D Purvis III and Rodney J Bartlett. A full coupled-cluster singles and doubles model: The inclusion of disconnected triples. *The Journal of chemical physics*, 76(4):1910–1918, 1982.
- [30] Jozef Noga and Rodney J Bartlett. The full CCSDT model for molecular electronic structure. *The Journal of chemical physics*, 86(12):7041–7050, 1987.
- [31] Fabian M Faulstich and Mathias Oster. Coupled cluster theory: Toward an algebraic geometry formulation. *SIAM Journal on Applied Algebra and Geometry*, 8(1):138–188, 2024.
- [32] Fabian M Faulstich, Bernd Sturmfels, and Svala Sverrisdóttir. Algebraic varieties in quantum chemistry. *Foundations of Computational Mathematics*, pages 1–32, 2024.
- [33] Svala Sverrisdóttir and Fabian M Faulstich. Exploring ground and excited states via single reference coupled-cluster theory and algebraic geometry. *Journal of Chemical Theory and Computation*, 20(19):8517–8528, 2024.
- [34] Josef Paldus. Correlation problems in atomic and molecular systems. v. spin-adapted coupled cluster many-electron theory. *The Journal of Chemical Physics*, 67(1):303–318, 1977.

- [35] Ruben Pauncz. *Spin eigenfunctions: construction and use*. Springer Science & Business Media, 2012.
- [36] Tomislav P Živković and Hendrik J Monkhorst. Analytic connection between configuration–interaction and coupled-cluster solutions. *Journal of Mathematical Physics*, 19(5):1007–1022, 1978.
- [37] J Paldus, P Piecuch, L Pylypow, and B Jeziorski. Application of hilbert-space coupled-cluster theory to simple $(H_2)_2$ model systems: Planar models. *Physical Review A*, 47(4):2738, 1993.
- [38] Piotr Piecuch, Sohrab Zarrabian, Josef Paldus, and Jiří Čížek. Coupled-cluster approaches with an approximate account of triexcitations and the optimized-inner-projection technique. ii. coupled-cluster results for cyclic-polyene model systems. *Physical Review B*, 42(6):3351, 1990.
- [39] Karol Kowalski and Karol Jankowski. Towards complete solutions to systems of non-linear equations of many-electron theories. *Physical Review Letters*, 81(6):1195, 1998.
- [40] Piotr Piecuch and Karol Kowalski. In search of the relationship between multiple solutions characterizing coupled-cluster theories. In J. Leszczynski, editor, *Computational Chemistry, Reviews of Current Trends*, pages 1–104. 2000.
- [41] Karol Kowalski and Piotr Piecuch. Complete set of solutions of multireference coupled-cluster equations: The state-universal formalism. *Physical Review A*, 61(5):052506, 2000.
- [42] Csirik, Mihály A. and Laestadius, Andre. Coupled-cluster theory revisited – part i: Discretization. *ESAIM: Mathematical Modelling and Numerical Analysis*, 57(2):645–670, 2023.
- [43] Mihály A Csirik and Andre Laestadius. Coupled-cluster theory revisited – part ii: Analysis of the single-reference coupled-cluster equations. *ESAIM: Mathematical Modelling and Numerical Analysis*, 57(2):545–583, 2023.
- [44] K Kowalski and P Piecuch. Complete set of solutions of the generalized bloch equation. *International Journal of Quantum Chemistry*, 80(4-5):757–781, 2000.
- [45] K Kowalski and K Jankowski. Full solution to the coupled-cluster equations: the H4 model. *Chemical Physics Letters*, 290(1-3):180–188, 1998.
- [46] K Jankowski and K Kowalski. Physical and mathematical content of coupled–cluster equations: Correspondence between coupled–cluster and configuration–interaction solutions. *The Journal of Chemical Physics*, 110(8):3714–3729, 1999.
- [47] K Jankowski and K Kowalski. Physical and mathematical content of coupled-cluster equations. ii. on the origin of irregular solutions and their elimination via symmetry adaptation. *The Journal of Chemical Physics*, 110(19):9345–9352, 1999.

- [48] K Jankowski and K Kowalski. Physical and mathematical content of coupled-cluster equations. iii. model studies of dissociation processes for various reference states. *The Journal of Chemical Physics*, 111(7):2940–2951, 1999.
- [49] K Jankowski and K Kowalski. Physical and mathematical content of coupled-cluster equations. iv. impact of approximations to the cluster operator on the structure of solutions. *The Journal of Chemical Physics*, 111(7):2952–2959, 1999.
- [50] Viktoriia Borovik, Bernd Sturmels, and Svala Sverrisdóttir. Coupled cluster degree of the Grassmannian. *Journal of Symbolic Computation*, 128:102396, 2025.
- [51] Svala Sverrisdóttir. Algebraic varieties in second quantization. *arXiv preprint arXiv:2505.17276*, 2025.
- [52] Reinhold Schneider. Analysis of the projected coupled cluster method in electronic structure calculation. *Numerische Mathematik*, 113(3):433–471, 2009.
- [53] Thorsten Rohwedder. The continuous coupled cluster formulation for the electronic schrödinger equation. *ESAIM: Mathematical Modelling and Numerical Analysis*, 47(2):421–447, 2013.
- [54] Thorsten Rohwedder and Reinhold Schneider. Error estimates for the coupled cluster method. *ESAIM: Mathematical Modelling and Numerical Analysis*, 47(6):1553–1582, 2013.
- [55] Andre Laestadius and Simen Kvaal. Analysis of the extended coupled-cluster method in quantum chemistry. *SIAM Journal on Numerical Analysis*, 56(2):660–683, 2018.
- [56] Andre Laestadius and Fabian M Faulstich. The coupled-cluster formalism—a mathematical perspective. *Molecular Physics*, 117(17):2362–2373, 2019.
- [57] Fabian M Faulstich, Andre Laestadius, Örs Legeza, Reinhold Schneider, and Simen Kvaal. Analysis of the tailored coupled-cluster method in quantum chemistry. *SIAM Journal on Numerical Analysis*, 57(6):2579–2607, 2019.
- [58] Muhammad Hassan, Yvon Maday, and Yipeng Wang. Analysis of the single reference coupled cluster method for electronic structure calculations: the full-coupled cluster equations. *Numerische Mathematik*, 155(1-2):121–173, 2023.
- [59] Muhammad Hassan, Yvon Maday, and Yipeng Wang. Analysis of the single reference coupled cluster method for electronic structure calculations: The discrete coupled cluster equations. *arXiv:2311.00637*, 2023.
- [60] Fabian M Faulstich. Recent mathematical advances in coupled cluster theory. *International Journal of Quantum Chemistry*, 124(13):e27437, 2024.
- [61] David Gontier, Antoine Levitt, and Sami Siraj-Dine. Numerical construction of Wannier functions through homotopy. *Journal of Mathematical Physics*, 60(3), 2019.

- [62] Éric Cancès, Alfred Kirsch, and Solal Perrin-Roussel. A mathematical analysis of IPT-DMFT. *arXiv preprint arXiv:2406.03384*, 2024.
- [63] Pavel Pokhilko and Dominika Zgid. Homotopy continuation method for solving dyson equation fully self-consistently: theory and application to NdNiO₂. *arXiv preprint arXiv:2507.00290*, 2025.
- [64] Stuart M Harwood, Dimitar Trenev, Spencer T Stober, Panagiotis Barkoutsos, Tanvi P Gujarati, Sarah Mostame, and Donny Greenberg. Improving the variational quantum eigensolver using variational adiabatic quantum computing. *ACM Transactions on Quantum Computing*, 3(1):1–20, 2022.
- [65] Viktoriia Borovik, Hannah Friedman, Serkan Hoşten, and Max Pfeffer. Numerical algebraic geometry for energy computations on tensor train varieties. *arXiv preprint arXiv:2512.06939*, 2025.
- [66] Erwin Schrödinger. An undulatory theory of the mechanics of atoms and molecules. *Physical review*, 28(6):1049, 1926.
- [67] J. Robert Oppenheimer Max Born. Zur quantentheorie der moleküle. *Annalen der Physik*, 389(20):457–484, 1927.
- [68] Jun John Sakurai and Jim Napolitano. *Modern quantum mechanics*. Cambridge University Press, 2020.
- [69] Wolfgang Pauli. Über den zusammenhang des abschlusses der elektronengruppen im atom mit der komplexstruktur der spektren. *Zeitschrift für Physik*, 31(1):765–783, 1925.
- [70] Vladimir Fock. Konfigurationsraum und zweite quantelung. *Zeitschrift für Physik*, 75(9):622–647, 1932.
- [71] Jean Gallier and Jocelyn Quaintance. Differential geometry and Lie groups, a second course, no. 13 in geometry and computing, 2020.
- [72] Trygve Helgaker, Poul Jorgensen, and Jeppe Olsen. *Molecular electronic-structure theory*. John Wiley & Sons, 2013.
- [73] Paul Adrien Maurice Dirac. The quantum theory of the emission and absorption of radiation. *Proceedings of the Royal Society of London. Series A, Containing Papers of a Mathematical and Physical Character*, 114(767):243–265, 1927.
- [74] P. Jordan and E. Wigner. Über das paulische äquivalenzverbot. *Zeitschrift für Physik*, 47:631–651, 1928.
- [75] Leon Armenovich Takhtadzhian. *Quantum mechanics for mathematicians*, volume 95. American Mathematical Soc., 2008.

- [76] Josef Paldus, Jiří Čížek, and Isaiah Shavitt. Correlation problems in atomic and molecular systems. iv. extended coupled-pair many-electron theory and its application to the B H 3 molecule. *Physical Review A*, 5(1):50, 1972.
- [77] William Fulton and Joe Harris. *Representation theory: a first course*, volume 129. Springer Science & Business Media, 2013.
- [78] W v Pauli Jr. Zur quantenmechanik des magnetischen elektrons. *Zeitschrift für Physik*, 43(9):601–623, 1927.
- [79] Walter Greiner and Bernd Müller. *Quantum Mechanics: Symmetries*. Springer, 1994.
- [80] Mateusz Michałek and Bernd Sturmfels. *Invitation to nonlinear algebra*, volume 211. American Mathematical Soc., 2021.
- [81] Fritz Coester. Bound states of a many-particle system. *Nuclear Physics*, 7:421–424, 1958.
- [82] Abigail Price, Ada Stelzer, and Svala Sverrisdóttir. Plane partitions and spin adapted quantum states. *arXiv preprint arXiv:2601.06295*, 2026.
- [83] Alexander P Morgan and Andrew J Sommese. Coefficient-parameter polynomial continuation. *Applied Mathematics and Computation*, 29(2):123–160, 1989.
- [84] Paul Breiding, Kathlén Kohn, and Bernd Sturmfels. *Metric algebraic geometry*. Springer Nature, 2024.
- [85] Paul Breiding and Sascha Timme. HomotopyContinuation.jl: A Package for Homotopy Continuation in Julia. In *Mathematical Software–ICMS 2018: 6th International Conference, South Bend, IN, USA, July 24–27, 2018, Proceedings* 6, pages 458–465. Springer, 2018.
- [86] Qiming Sun. Libcint: An efficient general integral library for Gaussian basis functions. *Journal of computational chemistry*, 36(22):1664–1671, 2015.
- [87] Qiming Sun, Timothy C Berkelbach, Nick S Blunt, George H Booth, Sheng Guo, Zhen-dong Li, Junzi Liu, James D McClain, Elvira R Sayfutyarova, Sandeep Sharma, et al. PySCF: the python-based simulations of chemistry framework. *Wiley Interdisciplinary Reviews: Computational Molecular Science*, 8(1):e1340, 2018.
- [88] Qiming Sun, Xing Zhang, Samragni Banerjee, Peng Bao, Marc Barbry, Nick S Blunt, Nikolay A Bogdanov, George H Booth, Jia Chen, Zhi-Hao Cui, et al. Recent developments in the PySCF program package. *The Journal of chemical physics*, 153(2), 2020.
- [89] Fabian M Faulstich, Vincenzo Galgano, Elke Neuhaus, and Irem Portakal. On the coupled cluster doubles truncation variety of four electrons. *To appear soon*.

- [90] Attila Szabo and Neil S Ostlund. *Modern quantum chemistry: introduction to advanced electronic structure theory*. Courier Corporation, 2012.
- [91] Curtis L Janssen and Ida MB Nielsen. New diagnostics for coupled-cluster and Møller–Plesset perturbation theory. *Chemical physics letters*, 290(4-6):423–430, 1998.
- [92] Ida M Beck Nielsen and Curtis L Janssen. Double-substitution-based diagnostics for coupled-cluster and Møller–Plesset perturbation theory. *Chemical physics letters*, 310(5-6):568–576, 1999.
- [93] Rodney J Bartlett, Young Choon Park, Nicholas P Bauman, Ann Melnichuk, Duminda Ranasinghe, Moneesha Ravi, and Ajith Perera. Index of multi-determinantal and multi-reference character in coupled-cluster theory. *The Journal of Chemical Physics*, 153(23), 2020.
- [94] Fabian M Faulstich, Håkon E Kristiansen, Mihaly A Csirik, Simen Kvaal, Thomas Bondo Pedersen, and Andre Laestadius. S-diagnostic – an a posteriori error assessment for single-reference coupled-cluster methods. *The Journal of Physical Chemistry A*, 127(43):9106–9120, 2023.
- [95] Robert S Mulliken. Electronic population analysis on LCAO–MO molecular wave functions. I. *The Journal of chemical physics*, 23(10):1833–1840, 1955.
- [96] RS Mulliken. Electronic population analysis on LCAO-MO molecular wave functions. III. effects of hybridization on overlap and gross ao populations. *The Journal of Chemical Physics*, 23(12):2338–2342, 1955.